

# Are Pt(IV) Prodrugs That Release Combretastatin A4 True Multi-action Prodrugs?

Claudia Schmidt,<sup>#</sup> Tomer Babu,<sup>#</sup> Hana Kostrhunova, Annika Timm, Uttara Basu, Ingo Ott,<sup>\*</sup> Valentina Gandin,<sup>\*</sup> Viktor Brabec,<sup>\*</sup> and Dan Gibson<sup>\*</sup>

Cite This: <https://doi.org/10.1021/acs.jmedchem.1c00706>

Read Online

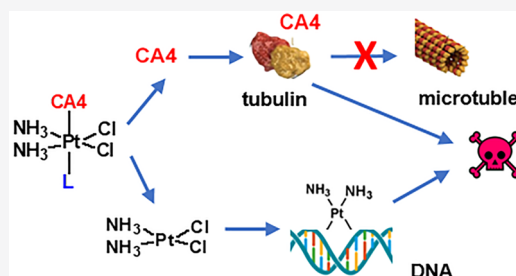
ACCESS |

Metrics & More

Article Recommendations

Supporting Information

**ABSTRACT:** “Multi-action” Pt(IV) derivatives of cisplatin with combretastatin A4 (CA4) bioactive ligands that are conjugated to Pt(IV) by carbonate are unique because the ligand ( $IC_{50} < 10$  nM) is dramatically 1000-folds more cytotoxic than cisplatin *in vitro*. The Pt(IV)-CA4 prodrugs were as cytotoxic as CA4 itself, indicating that the platinum moiety probably plays an insignificant role in triggering cytotoxicity, suggesting that the Pt(IV)-CA4 complexes act as prodrugs for CA4 rather than as true multi-action prodrugs. *In vivo* tests (Lewis lung carcinoma) show that *ctc*-[Pt(NH<sub>3</sub>)<sub>2</sub>(PhB)(CA4)Cl<sub>2</sub>] inhibited tumor growth by 93% compared to CA4 (67%), cisplatin (84%), and 1:1:1 cisplatin/CA4/PhB (85%) while displaying <5% body weight loss compared to cisplatin (20%) or CA4 (10%). In this case, and perhaps with other extremely potent bioactive ligands, platinum(IV) acts merely as a self-immolative carrier triggered by reduction in the cancer cell with only a minor contribution to cytotoxicity.



## INTRODUCTION

Chemotherapy is an important approach for the treatment of various cancers. Most chemotherapeutic protocols are not limited to a single drug (monotherapy) but rely on the combination of several drugs that act by different mechanisms against different cellular targets in the cancer cells (combination therapy).<sup>1,2</sup> This approach aims to overcome resistance by ensuring more efficient and complete killing of the cancer cells in a tumor.

Pt(II) complexes, such as cisplatin and its derivatives carboplatin or oxaliplatin (Figure 1), have been used worldwide in the clinic for the treatment of several types of cancers for more than 40 years.<sup>3</sup> These FDA-approved drugs, which exert their anticancer activity by binding to nuclear DNA, cause severe side effects that are due in part to their lack of stability under physiological conditions and lack of selectivity toward cancer cells. Most patients suffer from ototoxicity and nephrotoxicity, naming only the most common ones.<sup>4,5</sup> However, the major drawback is the high number of incidences of inherent resistance as well as resistance to the drugs that tumors develop during treatment.<sup>6</sup> Therefore, in order to overcome resistance, these platinum drugs are used in the clinic mostly in combination with other drugs with different potencies, toxicities, and modes of action to treat a variety of cancers.

Some examples of combination therapy with platinum drugs include the combination of paclitaxel and cisplatin for the treatment of several cancers;<sup>7</sup> folic acid, 5-fluorouracil, and oxaliplatin are combined in a three-component protocol (FOLFOX) for the treatment of colorectal cancer;<sup>8</sup> and FOLFIRINOX is a protocol that combines four drugs (folic

acid, 5-fluorouracil, irinotecan, and oxaliplatin) to treat pancreatic cancer.<sup>9</sup> These drugs are administered individually, making it difficult to control the process since each drug has its own pharmacokinetic profile and its own toxicity pattern.

In the last 2 decades, octahedral Pt(IV) complexes emerged as promising candidates for overcoming resistance. The relative stability of the low-spin  $d^6$  octahedral Pt(IV) complexes to substitution reactions means that they are less reactive toward biomolecules outside the cells, increasing their chances of reaching the cancer cells intact. After crossing the cell membrane, they are activated by reduction, releasing the Pt(II) drugs in their active form as well as their axial ligands (Scheme 1).<sup>10–13</sup> This provides a mechanism for the concurrent release of a ratiometrically defined combination of bioactive moieties inside the cancer cell. When two or even more drugs which act on different cellular targets with different modes of action are simultaneously released in the cancer cell, we have multi-action prodrugs.<sup>14–16</sup> This approach provides us with the opportunity to design a larger number of structural alterations compared to the square-planar Pt(II) complexes and resulted in the synthesis and evaluation of a large variety of Pt(IV) prodrugs whose activity is based on the activation-by-reduction concept.

Received: April 19, 2021

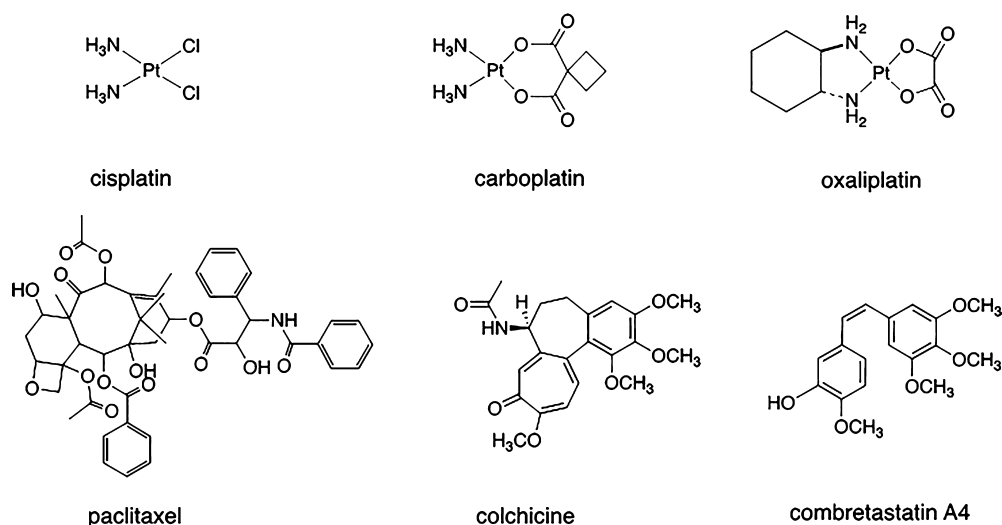


Figure 1. FDA-approved Pt(II) drugs—cisplatin, carboplatin, and oxaliplatin (top). Tubulin inhibitors (bottom).

Scheme 1. Pt(IV) Prodrugs Are Stable Outside the Cell and Are Activated by Reduction in the Cell Releasing the Pt(II) Drug That Binds to DNA as Well as the Two Axial Ligands

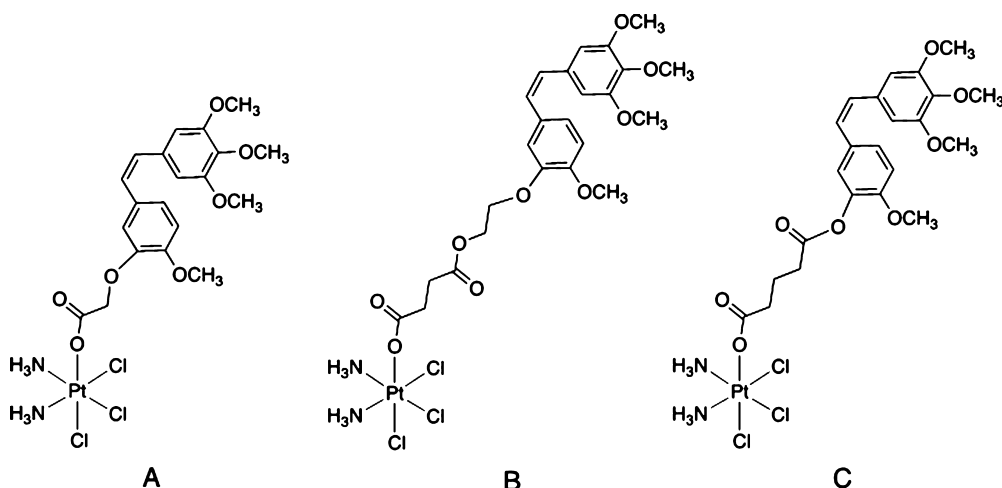
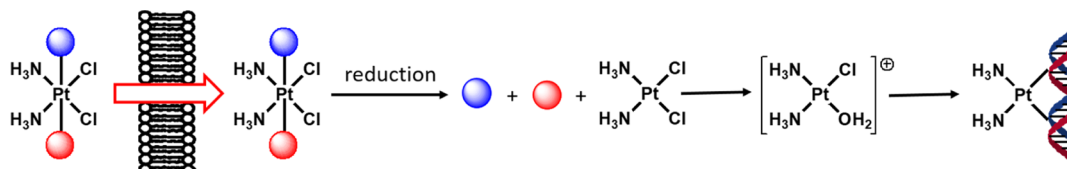


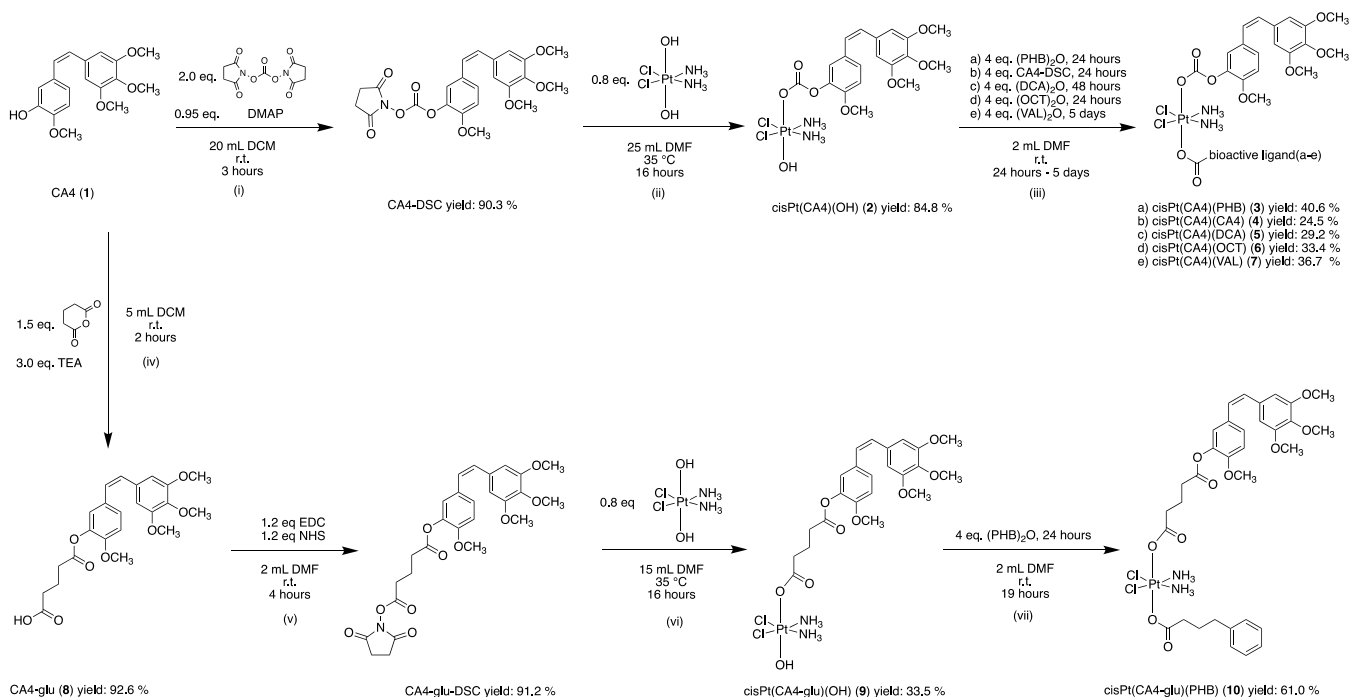
Figure 2. Pt(IV) complexes that were tethered to the axial OH with linkers that are not likely to release the free CA4 following reduction.<sup>23–25</sup>

Another class of potent anticancer drugs are the antimetabolic agents that disrupt the formation of the mitotic spindle. Drugs of this family include paclitaxel, docetaxel, colchicine, vincristine, and vinblastine that are often combined with Pt-based drugs (Figure 1).<sup>17</sup> In this context, we chose to explore the combination of cisplatin with the bioactive *cis*-stilbene combretastatin A4 (CA4) (Figure 1), that is an antimetabolic, antiangiogenic, and antiproliferative molecule first isolated from an African tree, called *Combretum caffrum*.<sup>18</sup> CA4 is a tubulin polymerization inhibitor of colchicine type.<sup>19,20</sup> Due to the antiangiogenic properties of the 4-O-phosphate derivative CA-4P (formally known as fosbretabulin), the compound is undergoing phase II/III clinical investigations against anaplastic thyroid cancer in combination with carboplatin and paclitaxel.<sup>21</sup>

Unfortunately, the three-drug combination did not show any advantages over the administration of carboplatin and paclitaxel alone. Considering that the three drugs have all different pharmacokinetics, combining two bioactive molecules in one complex might result in a higher activity and a lower overall toxicity as we have already shown in our latest report on a new Pt(IV) complex that combined cisplatin and gemcitabine.<sup>22</sup>

There are several reports describing the Pt(IV) conjugates of CA4. Because CA4 does not have a carboxylate that can be directly conjugated to Pt(IV), it had to be modified, and linkers, which included a carboxylate, were appended to CA4 so that it could be tethered to the OH of the Pt(IV). The linkers were conjugated to CA4 by stable ether or ester linkages (Figure 2).<sup>23–25</sup> The bonds between the linker and CA4 are fairly stable

## Scheme 2. Synthetic Schemes for the Preparation of Compounds



under physiological conditions, suggesting that following reduction the linker is likely to remain tethered to CA4 and that the released bioactive agent is the CA4-linker conjugate rather than free CA4.

Since even minor structural alterations of the bioactive molecule can influence the activity of a compound, we decided to synthesize and study the anticancer properties of a series of carbonate-linked Pt(IV)-CA4 complexes, which release the unmodified free CA4 after reduction. Moreover, we wanted to explore the effect of adding another bioactive ligand to the second axial position, forming “triple-action” prodrugs<sup>16</sup> on the pharmacological properties of the prodrugs. We chose the following compounds that have all shown to act synergistically with cisplatin: the HDAC inhibitors phenylbutyrate (PhB)<sup>14</sup> and valproate (Val)<sup>26</sup> as well as the PDK inhibitor dichloroacetate (DCA)<sup>27</sup> or octanoate (Oct) that enhances DNA methylation.<sup>28</sup> We investigated the influence of the trans axial ligands on the stability, rates of reduction, and cytotoxicity of these complexes and compared a carbonate-linked compound to its carboxylate-linked counterpart where CA4 was linked to the metal by a glutaric (glu) linker (Figure 2C). Biological investigations on the antiproliferative effects on a panel of different cancer cells were conducted and cellular uptake studies in MDA-MB-231 breast carcinoma cells were performed. *In vivo* studies in Lewis lung carcinoma mice were carried out to assess their tumor growth inhibition effects and overall toxicity (indicated by body weight loss) in comparison to the single application of the reference drugs cisplatin and CA4 and their co-administration.

## RESULTS & DISCUSSION

### Synthesis and Characterization of the Compounds.

Recently, we reported for the first time on a strategy for tethering ligands with an OH group to Pt(IV) such that following reduction of Pt(IV), the original ligands are released.<sup>22</sup> We accomplished this by attaching a hydroxyl group of a bioactive

molecule to the axial position of Pt(IV) via a carbonate. Following reduction of the Pt(IV) complex, the carbonate linker loses the non-toxic CO<sub>2</sub>, thereby generating the bioactive molecule in its original unaltered form. These designs tremendously extend the possibilities for new combinations of Pt(IV) complexes.

Our goal was to prepare multi-action Pt(IV) prodrugs where CA4 is conjugated to the axial position of Pt(IV) via a carbonate linkage in order to ensure that following the reduction of Pt(IV), and loss of CO<sub>2</sub>, CA4 will be released in the cell in its native form. The synthetic approach we adopted is similar to the one we described recently and is depicted in Scheme 2. We activated the hydroxyl of CA4 by reacting CA4 with *N,N*-disuccinimidyl carbonate (DSC) in the presence of *N,N*-dimethylpyridine-4-amine (DMAP) in dichloromethane (DCM) for 3 h. Stirring the reaction for more than 3 h or adding more equivalents of base resulted in the formation of a CA4 dimer, where two CA4 molecules are connected through a carbonate linker as the major product. The activated CA4 was reacted with oxoplatin to obtain the dual-action prodrug— $\text{cisPt}(\text{CA4})(\text{OH})$ , compound 2, in good yield (85%). Compound 2 also served as the precursor for the synthesis of the triple-action compounds 3–7 that were obtained by carboxylation of the axial OH of 2 with the appropriate anhydrides (Scheme 2).

While it is intellectually appealing and synthetically challenging to be able to modify the OH of CA4 in a way that following activation of the prodrug CA4 will be released in its free form, several studies demonstrated that the 3'-OH group of the B-ring is not essential for the interaction of CA4 with tubulin, and derivatives of CA4 where the OH was modified can retain good cytotoxicity.<sup>29</sup> Thus, for comparison, we also prepared the complex,  $\text{cisPt}(\text{CA4-glu})(\text{OH})$ , where CA4 was first modified with glutarate that was then activated with EDC and NHS and conjugated to the axial OH of Pt(IV), from which the triple-action derivative  $\text{cisPt}(\text{CA4-glu})(\text{PhB})$  was prepared (Scheme 2).

All complexes were characterized by  $^1\text{H}$ ,  $^{13}\text{C}$ , and  $^{195}\text{Pt}$ -NMR as well as by ESI mass spectrometry, and high purity was confirmed by high-performance liquid chromatography (HPLC) measurements and elemental analysis. The obtained data were consistent with the proposed structures (Supporting Information).

**Stability of the Compounds.** The stability of compounds 2, 3, 4, and 9 was measured by monitoring the decrease of the peak of the starting material by reversed-phase HPLC (RP-HPLC) in ACN/phosphate buffer, in ACN/cell culture medium, at 37 °C and following the reviewers' suggestion also in 1% dimethyl sulfoxide (DMSO)/cell culture medium. The results are presented in Table 1. The cisPt(CA4-glu)(OH)

**Table 1. Reduction and Stability Studies of Pt(IV) Complexes**

compound	stability studies			reduction studies
	$t_{1/2}$ in buffer (50%; ACN)	$t_{1/2}$ medium (50% ACN)	$t_{1/2}$ medium (1% DMSO)	$t_{1/2}$ in buffer (50% ACN)
(2) cisPt(CA4)(OH)	~3.5 days	~3 days	~1 day	9 min
(3) cisPt(CA4)(PhB)	~10 h	~4 h	~3 h	210 min
(4) cisPt(CA4)(CA4)	~1 h	~3 h	~2.5 h	27 min
(9) cisPt(CA4-glu)(OH)	>21 days	~12 days	~4 days	110 min
(10) cisPt(CA4-glu)(PhB)	>23 days	~11 days	~4.5 days	260 min

complex is very stable with half-lives >21 and ~12 days in buffer and medium, respectively. The higher stability of cisPt(CA4-

glu)(OH) and cisPt(CA4-glu)(PhB) compared to compounds 2, 3, and 4 is probably because carbonate linkers are more susceptible to hydrolysis than carboxylates.<sup>15</sup> The rate of hydrolysis of the axial CA4 seems to depend on the nature of the axial ligand trans to the carbonate. When the trans ligand is also a carbonate (4), the hydrolysis is fast, it is moderate when the trans ligand is carboxylate (3), and slow when it is OH (2). Interestingly, the hydrolysis in medium is faster than in buffer for cisPt(CA4)(PhB), slower for cisPt(CA4)(CA4), and still slow (>1 day) for cisPt(CA4)(OH) and of course for cisPt(CA4-glu)(OH) and cisPt(CA4-glu)(PhB). There are some differences between the half-lives measured in ACN/cell culture medium and 1% DMSO/cell culture medium particularly for cisPt(CA4)(OH), but the trend is the same.

**Reduction of the Compounds.** The rates of reduction of compounds 2, 3, and 4 were measured by HPLC in a 10-fold excess of an ascorbic acid solution in phosphate buffer (50 mM, pH 7.0). As expected, the dual-action compound, 2, was reduced rapidly due to the efficient electron transfer from ascorbate to Pt(IV)— $t_{1/2} = 9$  min. The bis-carbonate complex (4) had a  $t_{1/2}$  of 27 min and compound 3 had a  $t_{1/2}$  of 210 min. The relatively short half-life of cisPt(CA4)(CA4) could be due to the combination of hydrolysis, followed by the rapid reduction of cisPt(CA4)(OH). Because the retention times of CA4-glu and CA4 were identical, we could not use HPLC to verify whether the reduction product was CA4 or CA4-glu. Therefore, we characterized the reduction products of cisPt(CA4)(OH) and cisPt(CA4-glu)(OH) by  $^1\text{H}$  NMR spectroscopy in DMSO- $d_6$  with a 10-fold excess of ascorbate. As can be seen in Figure 3, the chemical shifts of free CA4 fall in the range of 6.3–6.9 ppm, while when bound to Pt(IV), these resonances are shifted

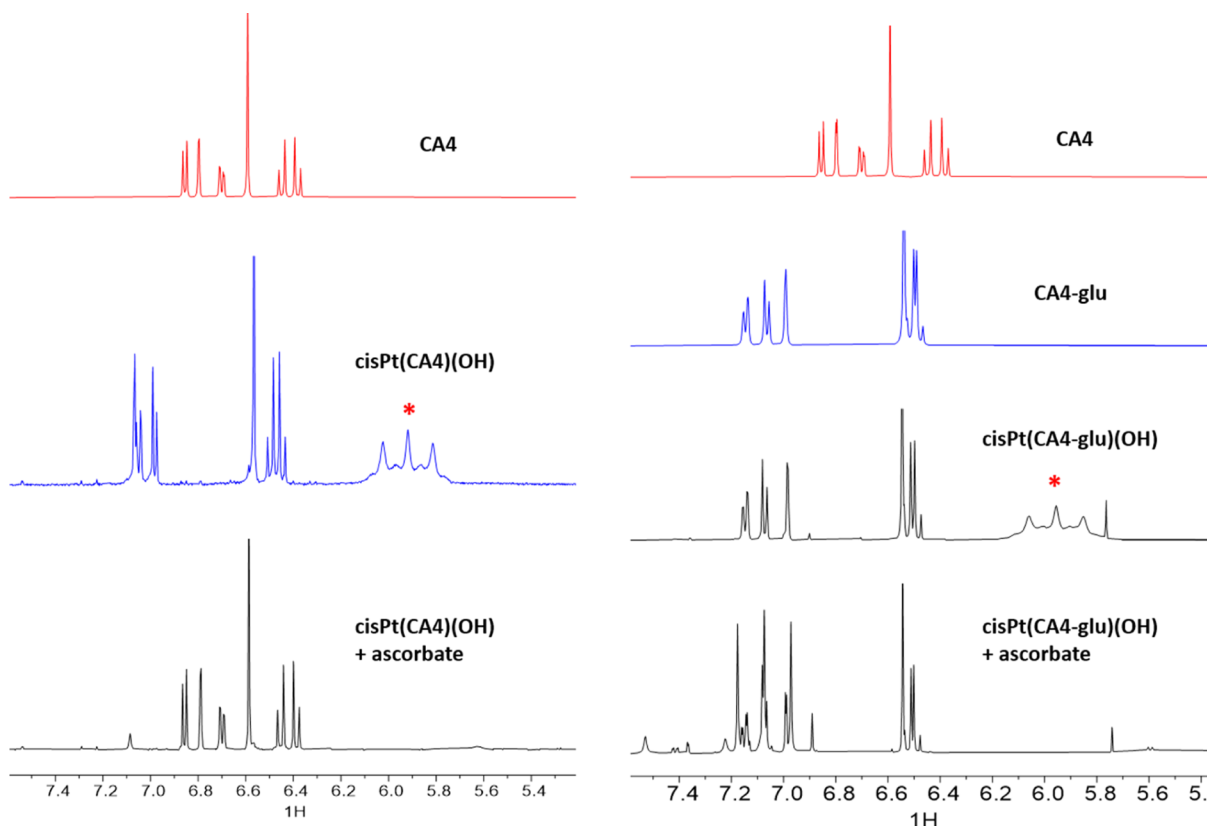


**Figure 3.** Reduction of carbonate vs carboxylate Pt(IV) complexes by ascorbic acid in DMSO- $d_6$  ( $^1\text{H}$  NMR 500 MHz).

**Table 2.** Antiproliferative Effects of Pt(IV)-CA4 Complexes on a Panel of Different Human Tumor Cells and a Healthy Human Kidney Cell Line<sup>a</sup>

compound	A2780 ovary	A2780cis ovary	A375 melanoma	PC9 lung	HT-29 colon	MCF-7 breast	MDA-MB-231 breast	SK-HEP-1 liver	RC-124 kidney	unit
cisplatin	2.41 (0.20)	26.46 (3.68)	3.08 (1.54)	9.94 (1.34)	7.99 (1.38)	10.65 (1.04)	8.83 (1.58)	28.00 (2.12)	1.04 (0.14)	$\mu$ M
1 + cisPt (1:1)	2.40 (0.41)	2.53 (0.31)	2.64 (0.04)	3.33 (0.11)	415.00 (15.56)	3.40 (0.53)	3.55 (0.16)	4.83 (0.56)	10.22 (0.49)	nM
1 + cisPt (2:1)	1.04 (0.09)	1.11 (0.04)	1.07 (0.35)	1.50 (0.14)	192.30 (3.99)	1.67 (0.22)	1.89 (0.28)	2.49 (0.26)	4.45 (0.37)	nM
1	2.37 (0.44)	2.80 (0.03)	2.02 (0.81)	4.64 (0.49)	348.21 (14.28)	3.14 (0.32)	3.68 (0.58)	3.00 (0.29)	9.31 (1.06)	nM
2	3.61 (0.78)	4.47 (0.64)	3.25 (1.04)	5.82 (1.27)	211.38 (5.62)	2.49 (0.35)	3.51 (0.11)	4.74 (0.18)	9.62 (1.90)	nM
3	4.01 (0.36)	4.52 (0.60)	3.52 (0.85)	6.78 (0.52)	101.96 (9.50)	2.77 (0.08)	3.19 (0.33)	4.02 (0.76)	11.11 (0.84)	nM
4	2.03 (0.29)	2.46 (0.67)	1.72 (0.78)	4.48 (0.88)	202.79 (1.53)	1.68 (0.23)	1.82 (0.18)	2.42 (0.10)	5.00 (1.28)	nM
5	3.64 (0.18)	3.87 (0.33)	2.47 (0.98)	5.89 (0.65)	1100 (370)	3.33 (0.37)	3.12 (0.37)	4.39 (0.47)	9.73 (0.72)	nM
6	4.18 (0.56)	4.58 (0.85)	3.94 (0.88)	7.18 (1.76)	139.90 (2.54)	3.66 (0.43)	4.37 (0.16)	5.62 (0.81)	7.84 (0.08)	nM
7	5.01 (1.19)	5.61 (1.26)	4.34 (1.58)	9.26 (1.41)	299.73 (7.95)	3.91 (0.18)	4.21 (0.35)	5.76 (0.87)	14.46 (0.71)	nM
8	1.78 (0.12)	1.68 (0.05)	1.76 (0.13)	2.29 (0.17)						nM
9	2.03 (0.11)	2.45 (0.43)	2.23 (0.66)	3.12 (0.15)						nM

<sup>a</sup>Cells were incubated for 72 h at 37 °C. (*n* = 3).

downfield and fall between 6.4 and 7.2 ppm. Once the Pt(IV) is reduced, as evidenced by the disappearance of the peak of the ammine ligands (triplet at 5.9 ppm—red asterisk), the aromatic peaks correspond to those of unbound free CA4. In contrast, the reduction of cisPt(CA4-glu)(OH), even after 48 h, does not show any signs of free CA4.

Interestingly, even the two most stable compounds both in buffer and in medium were reduced rather rapidly, lending support to the hypothesis that the prodrugs are relatively stable outside the cells and undergo rapid activation inside the cells.

**Antiproliferative Effects on Tumor Cells and Non-tumorigenic Cells.** The antiproliferative effect of the compounds was evaluated against a panel of eight cancer cell lines from different organs, both sensitive and resistant to cisplatin, and one non-tumorigenic human kidney cell line (RC-124). CA4 is a very potent cytotoxic agent with low nM IC<sub>50</sub> values in all the cancer cell lines and is about 1000-fold more potent than cisplatin. In contrast, the second axial ligands (Val, Oct, and PhB) are not cytotoxic on their own and have IC<sub>50</sub> values in the mM range against various cancer cell lines,<sup>14,26,28,30</sup> and the IC<sub>50</sub> values for DCA were reported as >100  $\mu$ M.<sup>27,31,32</sup> All the Pt(IV)-CA4 conjugates also exhibited low nM cytotoxicity (<10 nM) in all cancer cell lines with the exception of HT-29, where IC<sub>50</sub> values varied between 101 and 1100 nM (Table 2). The IC<sub>50</sub> values of the 1:1 and 2:1 mixture of CA4 and cisplatin reflect merely the IC<sub>50</sub> values of CA4 with no apparent contribution of cisplatin. Interestingly, there is no correlation between the IC<sub>50</sub> values of the compounds and their half-lives in culture cell medium, nor did we observe any dependence on the identity of the second bioactive ligand. The lack of correlation between stability in medium and the cytotoxicity is probably due to the fact that CA4 itself is so potent, so that even if a Pt(IV) compound is hydrolyzed or reduced in the medium, and CA4 is released before it enters the cell, CA4 itself will still exert its cytotoxic effect with the same efficacy. It is noteworthy that the nature of the linker between the OH of CA4 and Pt(IV), and consequently what is released in the cell, can significantly affect the potency of the prodrug. This was also noticeable in the case where the carbonate-linked gemcitabine, ctc-[Pt(NH<sub>3</sub>)<sub>2</sub>(Gem-carb)(PhB)Cl<sub>2</sub>], is significantly more cytotoxic than the succinate-linked gemcitabine, ctc-[Pt(NH<sub>3</sub>)<sub>2</sub>(Gem-suc)(PhB)Cl<sub>2</sub>].<sup>22</sup>

**Protein Binding of Platinum Complexes.** Binding to serum proteins, particularly albumin, can significantly affect the

efficacy of prodrugs in vivo. While direct covalent binding of cisplatin to albumin serves to inactivate the drug by reducing its bioavailability, the efficacy of Pt(IV) prodrugs can be enhanced by deliberately targeting (covalently<sup>33,34</sup> or non-covalently<sup>35</sup>) albumin in vivo, using it to deliver the cytotoxic agent to the tumor. One such compound, BTP-114, is in clinical trials.<sup>36</sup>

The binding of cisplatin, cisPt(CA4)OH, cisPt(CA4)(PhB), and cisPt(CA4-glu)(PhB), which were tested in vivo, to fetal calf serum (FCS) proteins (10 v/v %) in Dulbecco's modified Eagle's medium (DMEM) was evaluated over 24 h in an ethanol precipitation assay. The respective complexes were added to the medium, and aliquots were collected at different time points. Proteins were precipitated by the addition of ethanol. The unbound metal content was determined in the supernatant, and the metal bound to FCS proteins was calculated (%) and the results are depicted in Figure 4. The values for cisplatin are in

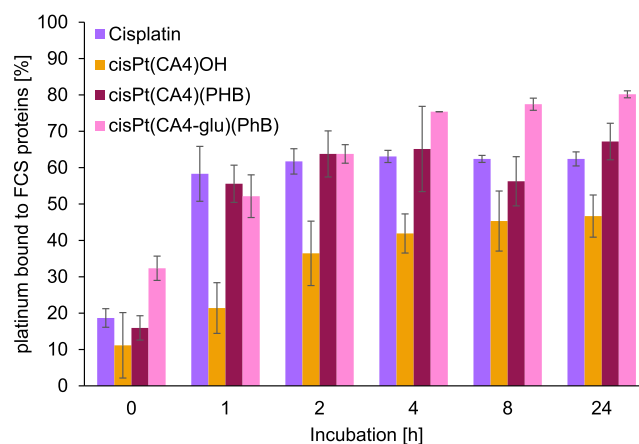


**Figure 4.** Platinum binding to FCS proteins in DMEM cell culture medium over 24 h at 37 °C.

accordance with the values reported in the literature.<sup>37</sup> Cisplatin and cisPt(CA4)(PhB) reach a plateau after 2 h of incubation, where 62–67% of the compound is bound to the proteins. The complex cisPt(CA4)(OH) binds slower and to a lower extent to proteins. After 8 h of incubation only, 45% was found to be bound to proteins. In contrast, cisPt(CA4-glu)(PhB) binds rapidly and to a larger extent to FCS proteins in comparison to

Table 3. Cellular Platinum Accumulation and DNA Platination in MDA-MB-231 Cells

	cellular uptake (ng Pt/10 <sup>6</sup> cells) <sup>a</sup>			DNA platination (pg Pt/μg DNA) <sup>b</sup>
	0.1 μM	1 μM	10 μM <sup>c</sup>	10 μM
oxoplatin		0.12 ± 0.02	1.1 ± 0.2	3.6 ± 0.8
cisplatin		0.8 ± 0.2	6 ± 1	7 ± 1
Pt(CA4)(OH)	0.14 ± 0.01	1.5 ± 0.4	15 ± 3	23 ± 3
Pt(CA4-glu)(OH)	0.29 ± 0.04	2.6 ± 0.3	18 ± 4	28 ± 2
Pt(CA4)(PhB)	0.5 ± 0.1	5 ± 1	68 ± 8	80 ± 10

<sup>a</sup>Cellular platinum accumulation into MDA-MB-231 cells after 5 h of exposure to 0.1, 1, or 10 μM of the compounds. <sup>b</sup>Platinum associated with DNA in MDA-MB-231 cells after 5 h of exposure to 10 μM of the compounds. <sup>c</sup>Cell viability at the time of harvesting as determined with trypan blue was not under 89%.

all the other platinum complexes. A plateau is reached after 4 h with a maximum of 80% platinum bound to FCS.

We presume that the binding of cisplatin to the proteins is covalent, while the Pt(IV) compounds are bound to the proteins non-covalently. In order to see whether lipophilicity affects the protein binding, we note that based on the retention times on a C18 column, under identical conditions, the order of lipophilicity is cis(CA4-glu)(PhB)—6.13 min > cis(CA4)(PhB) 6.11 min > cis(CA4)(OH) 4.69 min, indicating that a higher lipophilicity enhances the binding capabilities of the platinum complexes.

**Cell Uptake.** Before a metallodrug reaches its pharmacological target in the cell, it must first accumulate in cells. It has been demonstrated that a higher accumulation of metallodrugs generally potentiates antiproliferative activity. Moreover, the mechanism of action of antitumor metallodrugs is a multi-step process that includes as the first step cell entry or accumulation.<sup>38</sup> Therefore, the cellular levels of the investigated compounds were measured after a 5 h exposure of the MDA-MB-231 cells to the platinum complexes at concentrations 0.1 and 1.0 μM at 37 °C. The relatively high concentration (with respect to the IC<sub>50</sub> values) and short treatment time were chosen to balance the detection limit and the effort to evaluate cells in a viable state (cell viability at the moment of harvesting was above 90%). The platinum amount determined with inductively coupled plasma mass spectrometry (ICP-MS) was related to the cell counts. The accumulation of platinum from the investigated Pt(IV)-CA4 conjugates was approximately 1.9–6.3-fold greater than that from cisplatin, indicating that one factor responsible for the enhanced antiproliferative activity of Pt(IV)-CA4 conjugates in comparison with conventional cisplatin is their increased cellular accumulation (Table 3).

We also determined the accumulation of platinum from the investigated Pt(IV)-CA4 conjugates when the cellular levels of platinum from the investigated compounds were measured after exposure of the MDA-MB-231 cells to the platinum complexes at the considerably higher concentration (10 μM) when, however, the cell viability at the moment of harvesting was only around 89%. The results in Table 3 show that also under these conditions, the accumulation of platinum from the investigated Pt(IV)-CA4 conjugates was considerably greater than that from cisplatin (approximately 2.5–11.3-fold). Moreover, when the cells were treated with the investigated compounds at their elevated concentration (10 μM), it was also possible to measure platinum from these compounds associated with DNA isolated from the treated cells. The level of DNA platination correlated with the cellular platinum accumulation in MDA-MB-231 cells, that is, it was considerably greater in DNA isolated from the cells treated with Pt(IV)-CA4

conjugates than from the cells treated with cisplatin (approximately 3.3–11.7-fold).

**Tubulin Polymerization Inhibition in Cells.** CA4 is a tubulin-binding chemotherapy drug.<sup>39</sup> It interferes with the microtubule dynamics of tubulin acting as a tubulin polymerization inhibitor.<sup>40</sup> CA4 is known to bind the β-subunit of tubulin (colchicine site) and thus prevents cells from producing microtubules that are essential for cytoskeleton formation. Whole-cell flow cytometry analysis of microtubules was used previously to assess the ability of various compounds to alter tubulin/microtubule dynamics.<sup>41,42</sup> The method uses a mild lysis buffer and stabilization of microtubule network with glutaraldehyde. We employed this approach to investigate whether the investigated Pt(IV)-CA4 agents are able to modulate the tubulin/microtubule dynamics upon entering the cells (and presumably releasing the combretastatin unit). MDA-MB-231 cells were treated with a series of concentrations of CA4, CA4-glu, cisPt(CA4)(OH), and cisPt(CA4-glu)(OH) for 8 h. The cells were then harvested, fixed, and stained with an anti-α-tubulin-FITC antibody. It is expected that under these experimental conditions, compounds that effectively inhibit tubulin polymerization will show decreased fluorescence compared to the control. The results (Figure 5) demonstrate a significant and dose-dependent decrease in FITC fluorescence,

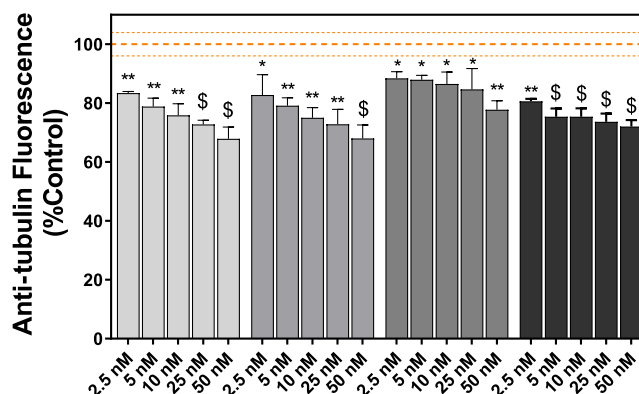


**Figure 5.** Microtubule analysis in cells. MDA-MB-231 cells were treated with indicated concentrations of the investigated compounds for 8 h, harvested, fixed, and stained with the anti-α-tubulin-FITC antibody. The fluorescence signal was normalized to the signal of non-treated control (orange lines: mean ± SD). Very light gray; light gray—CA4-glu; dark gray—cisPt(CA4)(OH); and black—cisPt(CA4-glu)(OH). The value of fluorescence of untreated control was taken as 100%. The data represent a mean of three independent experiments. The symbols \*/\*\*/\$ indicate a significant difference from the untreated control cells with  $p < 0.05$ ,  $p < 0.01$ , and  $p < 0.001$ , respectively, based on a two-tailed Student's *t*-test.

indicating a lower amount of polymerized tubulin mass in the cells treated with the investigated Pt(IV)-CA4 agents. Thus, the data support the view that the investigated Pt(IV)-CA4 agents can act through the inhibition of the tubulin polymerization similar to free CA4 and CA4-glu, although with slightly lower efficiency. Moreover, cisPt(CA4-glu)(OH) was more effective than cisPt(CA4)(OH), which likely reflects the lower cellular accumulation of cisPt(CA4)(OH) (Table 3). It is noteworthy that the cisPt(CA4) compounds significantly inhibit cellular tubulin polymerization at low nM concentrations that are in the same range as their IC<sub>50</sub> values. However, the level of DNA platination was observed under the conditions when a significant fraction of cells lost their viability. Thus, these results cannot be taken as a support for the view that the mechanism of action of Pt(IV) conjugates involves the processing of platinum–DNA adducts.

**Microtubule Imaging.** The microtubule network in MDA-MB-231 cells non-treated or treated with the tested compounds was visualized by immunofluorescence. The non-treated cells and cells treated with oxoplatin display a typical elongated spindle shape, whereas the treatment with agents containing the CA4 moiety induced changes in cell morphology, including condensation of the microtubule material near the cell surface, loss of membrane protrusions, and microtubule depolymerization (Figure 6).

**Tubulin Polymerization Inhibition in a Cell-Free Medium.** As cisPt(CA4)(OH) and cisPt(CA4-glu)(OH) inhibited cellular tubulin polymerization (Figure 5), we proceeded to find out the effect of Pt(IV)-CA4 compounds on *in vitro* tubulin polymerization. Purified tubulin was incubated in the absence and presence of different concentrations of CA4, CA4-glu, cisPt(CA4)(OH), cisPt(CA4-glu)(OH), and cisPt(CA4)(PhB), and the effect of the compounds on the polymerization of tubulin was monitored using the fluorescence-based tubulin polymerization assay kit (porcine tubulin; Cytoskeleton, Inc.). Thus, polymerization of porcine tubulin in the presence or absence of the investigated compounds was followed by an increase in fluorescence at 37 °C. Figure 7 shows that CA4 inhibited the tubulin assembly in a concentration-dependent manner with a significant effect visible at a concentration of CA4 at 1 μM. CA4-glu was considerably less effective, whereas the efficiency of cisPt(CA4)(OH), cisPt(CA4-glu)(OH), and cisPt(CA4)(PhB) at 1 μM concentration was almost negligible. These results suggest that the inhibition of tubulin polymerization inside the cell (Figure 5) was caused by CA4 released from cisPt-CA4 inside cells, although the intact cisPt-CA4 complexes might also contribute at least partially to the effect.

**Cell Cycle Analysis.** We investigated the cell cycle distribution of MDA-MB-231 cells treated with the investigated compounds for 24 h. The results are shown in Figure 8. Cisplatin and oxoplatin arrest the cells in the S phase with cisplatin causing more pronounced changes. All compounds containing the combretastatin moiety arrest the cells predominantly in the G2/M phase, which is typical for compounds which inhibit tubulin polymerization. The three compounds possessing platinum as well as combretastatin parts induce G2/M arrest; however, cell population in the S phase is increased as compared to the two no-platinum complexes.

**Role of Platinum in Inducing Cell Death.** The cytotoxicity data indicate that the Pt(IV)-CA4 complexes described here present an interesting example of combining cisplatin with a bioactive ligand that is 1000-fold more potent

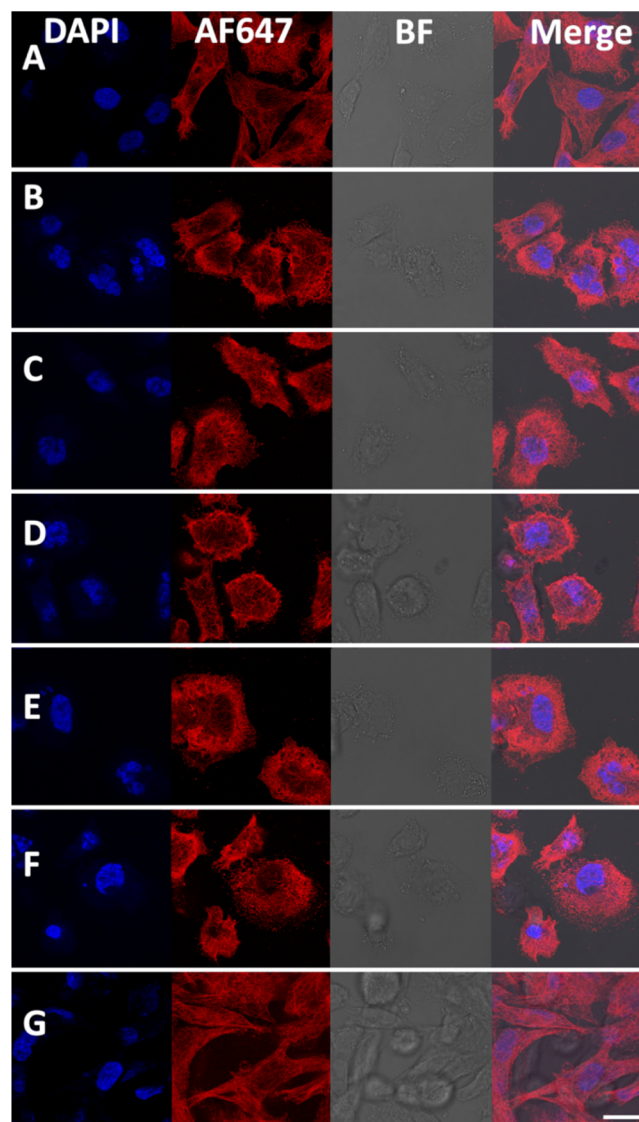


**Figure 6.** Effects of the investigated compounds on microtubule organization. MDA-MB-231 cells were incubated with the tested compounds at the concentrations corresponding to their IC<sub>50</sub> values (MTT, 72 h) for 24 h. Images were obtained with confocal microscopy of anti- $\alpha$ -tubulin immunofluorescence (red) preparations; DNA was stained with DAPI (blue). BF—bright field. (A) Control non-treated cells and (B–G) cells treated with individual compounds: (B) CA4, (C) CA4-glu, (D) cisPt(CA4)(OH), (E) cisPt(CA4-glu)(OH), (F) cisPt(CA4-glu)(PhB), and (G) oxoplatin. Scale bar represents 25 μm.

than cisplatin. Moreover, all the complexes, with the exception of cisplatin, have nearly identical IC<sub>50</sub> values in the low nM range, suggesting that CA4 rather than cisplatin is responsible for the killing of the cancer cells.

These results are markedly different from those reported for what looks like similar Pt(IV) derivatives of cisplatin where CA4 is conjugated to Pt(IV) via different linkers (Figure 2). For the prodrug in Figure 2A, the bioactive ligand (CA4 derivative) is 1.25–4.27-fold less potent than cisplatin in four out of five cancer cell lines, and the complex itself is only 2.58–11.31 times more potent than cisplatin, suggesting that both moieties contribute to cell death.<sup>23</sup> For the compound in Figure 2B, the bioactive ligand is 3.72–8.52-fold more potent than cisplatin and the complex is 11.78–21.83 times more potent than cisplatin.<sup>24</sup> The IC<sub>50</sub> value of the bioactive ligand in Figure 2C is

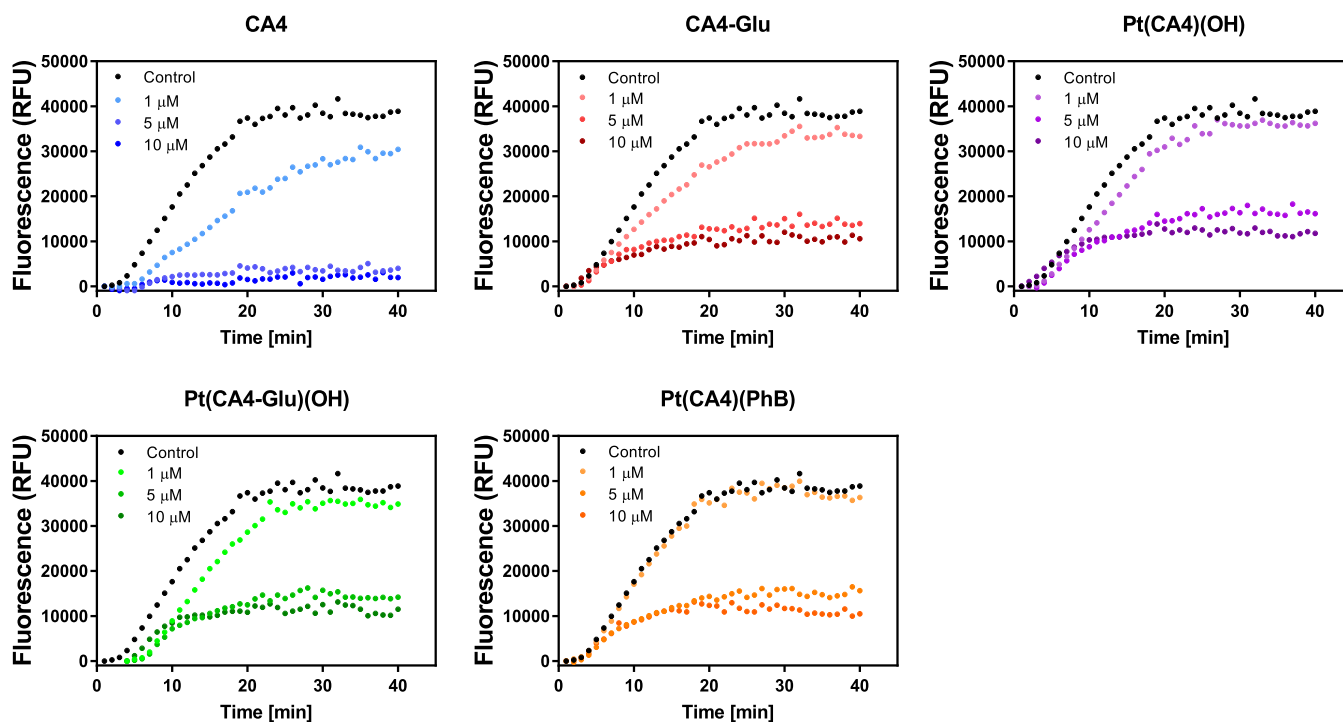


**Figure 7.** Tubulin assembly curves. Fluorescence-based tubulin polymerization assay kit was employed. Polymerization was recorded in the absence (black dots) or presence of the tested compounds at 37 °C.

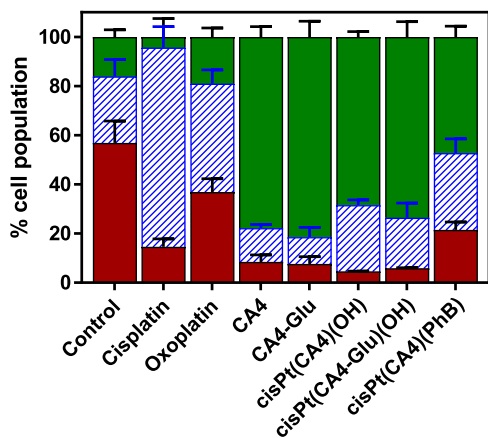


**Figure 8.** Cell cycle distribution of MDA-MB-231 cells following a 24 h exposure to individual compounds at concentrations corresponding to their respective  $IC_{50}$  values (MTT, 72 h). The cells were washed, fixed with 70% ethanol, stained with propidium iodide, and subjected to FACS analysis. Red—G1 phase, blue dashed region—S phase, and green—G2/M phase. The percentages of MDA-MB-231 cells corresponding to the individual phases of cell cycle were acquired with ModFit software and are expressed as mean  $\pm$  SD (three experiments).

not reported, but the complex has nearly identical  $IC_{50}$  values to CA4 in four cancer cell lines being 29.2–34.23-fold more potent than cisplatin. Interestingly, also the oxaliplatin and the Pt(DACH)Cl<sub>2</sub> analogues of this compound have nearly the same  $IC_{50}$  values as the cisplatin analogues, suggesting that activity might be due primarily to the bioactive ligand.<sup>25</sup> We also note that in the cell lines that we used, the  $IC_{50}$  of CA4 was in the low nM range (<10 nM), in agreement with several reports,<sup>29</sup> while the values reported for CA4 for the compounds in Figure 2 are in the 100–300 nM range.

Therefore, due to this unique case where there is a huge difference in potencies between the bioactive ligands and cisplatin, an obvious question is whether the released platinum (cisplatin) has a significant contribution toward the killing of the cancer cell. In order to answer this question, we first isolated DNA from MDA-MB-231 cells treated with Pt(IV)-CA4 compounds under similar conditions to those used for measuring cellular platinum accumulation in MDA-MB-231 cells treated with cisPt-CA4 compounds (Table 3), that is, a 5 h exposure of the MDA-MB-231 cells to the platinum complexes at concentrations 0.1 and 1.0  $\mu$ M or a 24 h exposure to the platinum complexes at a concentration of 0.01  $\mu$ M at 37 °C. However, under these conditions, no measurable platinum from cisPt-CA4 compounds was found to be associated with DNA.

These results can be interpreted to mean that DNA in the cells treated with cisPt-CA4 compounds was not modified by Pt adducts because the Pt moiety released from Pt-CA4 compounds did not reach the cell nucleus or that it entered the cell nucleus but did not bind covalently to the DNA or that its DNA adducts were efficiently repaired. Another eventuality is that due to the relatively low  $IC_{50}$  values of the investigated cisPt-CA4 compounds, we could only use in these experiments relatively low concentrations of the Pt compounds (to warrant that most of the cells used in this experiment were alive). Thus, the level of Pt associated with DNA might be so low that it was below the limit of detection by ICP–MS. Therefore, as we did in a number of our previous papers,<sup>28,43,44</sup> we also used an additional test that makes it possible to determine whether DNA is a target of the investigated compounds. This test is based on the fact that platinum drugs are more cytotoxic in cells deficient in DNA repair.<sup>45</sup> Mutant Chinese hamster ovary CHO-K1 cells MMC-2 deficient in DNA nucleotide excision repair were more sensitive (9.7- or 9.3-fold) to killing by cisplatin or oxoplatin compared with the wild-type cells (Table 4), consistent with the previously obtained results.<sup>45,46</sup> This result confirms that the

**Table 4. Antiproliferative Activity Data [IC<sub>50</sub> Mean Values] Obtained by MTT Test for Chinese Hamster Ovary CHO-K1 Cell Line (Wild Type) and Its Mutant Cell Line MMC-2 Deficient in DNA Repair<sup>a</sup>**

	unit	CHO-K1	MMC-2	F <sup>b</sup>
CA4	nM	6 ± 1	4.9 ± 0.8	1.2
oxoplatin	μM	40 ± 2	4.3 ± 0.5	9.3
cisplatin	μM	24 ± 4	2.5 ± 0.5	9.6
cisPt(CA4)(OH)	nM	5.3 ± 0.6	1.4 ± 0.2	3.8
cisPt(CA4-glu)(OH)	nM	5.8 ± 0.7	1.3 ± 0.3	4.5
cisPt(CA4)(PhB)	nM	4.5 ± 0.6	1.1 ± 0.3	4.1

<sup>a</sup>The drug treatment period was 72 h. The results are expressed as mean values ± SD from three independent experiments, each performed in triplicate. <sup>b</sup>F = factor defined as IC<sub>50</sub> (NER-efficient, CHO-K1)/IC<sub>50</sub> (NER-deficient, MMC-2).

important cellular target of the antiproliferative activity of cisplatin or oxoplatin is nuclear DNA.<sup>46</sup> Contrastingly, the antiproliferative activity of CA4 was almost identical in both cell lines, indicating that DNA is an unlikely target of the antiproliferative activity of CA4. CisPt(CA4)(OH), cisPt(CA4-glu)(OH), and cisPt(CA4)(PhB) were more active in MMC-2 cells (3.9-, 4.6-, and 4.2-fold, respectively) than in CHO-K1 cells; however, the difference in antiproliferative activities was not as pronounced as in the case of cisplatin and oxoplatin. This finding suggests that repairable DNA damage by the platinum moiety released from Pt-CA4 compounds may play a considerably less decisive role in the mechanism of their antiproliferative activity in comparison with cisplatin or oxoplatin.

**In Vivo Studies.** *In vitro* cytotoxicity studies are unfortunately scarcely effective in predicting the *in vivo* pharmacodynamics profile of a putative drug. Therefore, we took a step forward toward preclinical translational studies by performing preliminary *in vivo* anticancer investigations comparing cisplatin, CA4, cisPt(CA4)(PhB), cisPt(CA4)(OH), and cisPt(CA4-glu)(PhB) against the murine Lewis lung carcinoma (LLC) solid tumor model. Seven days after tumor inoculation, the tumor-bearing mice were randomized into vehicle control and treatment groups. Control mice received the vehicle, whereas treated groups received daily oral doses of Pt(IV) complexes (20 mg kg<sup>-1</sup>), daily *i.p.* of 3 mg kg<sup>-1</sup> of cisplatin, and 20 mg kg<sup>-1</sup> of CA4, 20 mg kg<sup>-1</sup> of PhB, or a combination of cisplatin, CA4 and PhB (3 mg/kg, ratio 1:1:1). The tumor growth was evaluated at day 15, and the results are summarized in Table S1. The changes in body weights were monitored at day 0 and from day 7 onward every 2 days as a sign of systemic toxicity (Figure 9).

PhB proved to be barely effective in reducing the tumor volume mass and CA4 induced a 67% reduction of tumor mass significantly lower compared to cisplatin (84%). The antitumor effect induced by cisPt(CA4)(OH) was comparable to that induced by cisplatin (84% inhibition), and, noteworthy, administration of cisPt(CA4-glu)(PhB) or cisPt(CA4)(PhB) determined a superior reduction of the tumor mass by 91.5 and 92.6%, respectively. The *i.p.* treatment with the combination of cisplatin, CA4, and PhB induced a tumor mass reduction that was comparable to that of cisplatin alone and significantly lower than that induced by the triple-acting compounds cisPt(CA4-glu)(PhB) and cisPt(CA4)(PhB). In addition, the time course

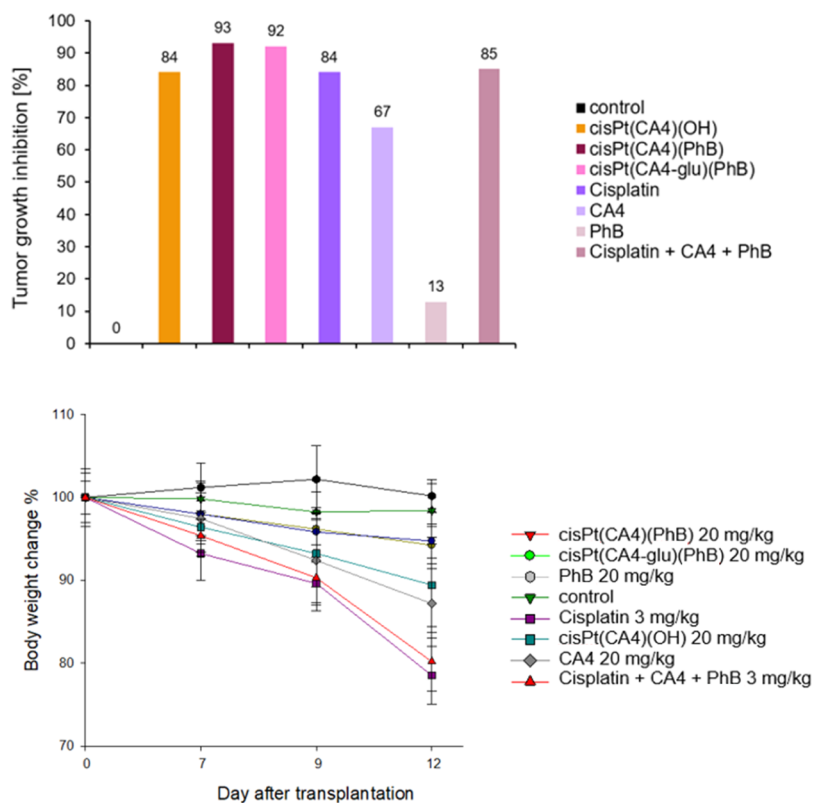


**Figure 9.** Top—Inhibition of tumor growth, days 7–14: animals received daily oral gavage of 20 mg kg<sup>-1</sup> of Pt(CA4)(PhB), Pt(CA4)(OH), or cisPt(CA4-glu)(PhB) and daily *i.p.* of 3 mg kg<sup>-1</sup> of cisplatin and 20 mg kg<sup>-1</sup> of CA4. At day 15, animals were sacrificed. Bottom—Body weight changes of LLC-bearing C57BL mice treated with the vehicle or the tested compounds. The error bars indicate SD.

of body weight changes attested that cisplatin and the i.p. drug combination induced elevated anorexia, whereas all Pt(IV) derivatives were significantly better tolerated by animals, inducing only minimal body weight loss (<10%) throughout the therapeutic experimentation. It is important to notice that combination treatment with higher doses of cisplatin, CA4, and PhB were discontinued due to elevated toxicity.

The compound reported in Figure 2A was previously tested *in vivo* by Li and co-workers in an HepG-2 tumor xenograft model and was compared to cisplatin, CA4, and 1:1 cisplatin/CA4. Similar to what we observed in our study, CA4 that was found to be most potent *in vitro* elicited the weakest *in vivo* anticancer activity.<sup>24</sup> However, in contrast to what we observed with compounds cisPt(CA4-glu)(PhB) and cisPt(CA4)(PhB), the complex in Figure 2A displayed inferior tumor inhibition compared to both cisplatin and the 1:1 mixture. The compound in Figure 2B was also previously tested against a SK-OV-3 xenograft model by Huang and collaborators, and in this case, the complex was somewhat more active than CA4 but less active than cisplatin or a combination of cisplatin and CA4.<sup>25</sup>

It is interesting to note that the “dual-action” compounds with either an OH, cisPt(CA4)(OH), or Cl axial ligands (Figure 2) were less efficacious than cisplatin *in vivo*, while the two “triple-action” compounds with the PhB ligand were significantly more active than cisplatin. Although cisPt(CA4)(OH) and cisPt(CA4)(PhB) have nearly identical IC<sub>50</sub> values *in vitro* and despite the fact that cisPt(CA4)(OH) is significantly more stable than cisPt(CA4)(PhB) in the cell culture medium, cisPt(CA4)(PhB) is significantly more active *in vivo*. This might be because the “dual-action” prodrugs, with the OH or Cl axial ligands, are reduced significantly faster than the “triple-action” prodrugs and perhaps they are reduced *in vivo* prior to reaching the tumor. Another possible explanation for the differences in efficacy and toxicity between the “triple-action” compounds, cisPt(CA4-glu)(PhB) and cisPt(CA4)(PhB), and cisPt(CA4)(OH) might be the ability of the former to interact non-covalently with albumin via PhB, resulting in higher stability and bioavailability.

## CONCLUSIONS

The results of these studies provide us with some interesting insights into Pt(IV) multi-action prodrugs. The prodrugs described here differ from most other reported Pt(IV) prodrugs because the free bioactive moiety (CA4) that is released inside the cancer cell, with low nanomolar IC<sub>50</sub> values, is dramatically (1000 fold) more cytotoxic than the platinum drug (low micromolar IC<sub>50</sub>). All six cisPt(CA4) “multi-action” prodrugs, regardless of the identity of the second bioactive ligand, have low nanomolar IC<sub>50</sub> values against seven out of the eight cancer cell lines, suggesting that CA4 is the dominant factor in triggering cell death, raising doubts whether platinum makes any significant contribution toward cell death. Comparison of the cytotoxicity data to that of similar compounds that were previously reported suggests that the nature of the link between the OH of CA4 and Pt(IV) significantly affects the pharmacological properties of the prodrugs. Comparing the IC<sub>50</sub> values of the compounds against a pair of cancer cells lines proficient and deficient in DNA repair (NER), we found that cisplatin and oxoplatin were about 9-fold more potent against cells deficient in DNA repair, while the cisPt(CA4) prodrugs were only about 4-fold more potent. This, in conjunction with our inability to detect by ICPMS Pt–DNA adducts in the nucleus, suggests that the small amount of cisplatin that is

released in the cancer cell probably makes only a limited contribution to the killing of the cancer cells. The *in vitro* data lead us to suggest that these compounds are not true multi-action cytotoxic agents but rather prodrugs of CA4.

Although the contribution of platinum to the killing of the cells *in vitro* is not clear, the conjugation of CA4 to Pt(IV) significantly enhanced the *in vivo* tumor inhibition and reduces the acute toxicity (weight loss) compared to CA4. Notably, CA4 that is the most potent *in vitro* is the least efficacious *in vivo*. The two most efficacious prodrugs, 3 and 8, inhibit tumor growth by ~92% compared to cisplatin (84%), CA4 (67%), and 1:1 cisplatin/CA4 (85%). This demonstrates again that the *in vitro* cytotoxicity does not necessarily translate to *in vivo* activity.

If indeed, CA4, rather the cisplatin, is primarily responsible for killing the cancer cells, what is the role of the platinum moiety? In this case, and perhaps in other cases of Pt(IV) complexes with extremely potent bioactive ligands, the main role of Pt(IV) is merely to act as a self-immolative carrier that is activated by reduction inside the cancer cell and serves to improve the efficacy of CA4 and reduce its acute toxicity.

While we usually think of Pt(IV) complexes as prodrugs whose task is to deliver the cytotoxic Pt(II) drugs (sometimes accompanied by other bioactive moieties) to the cancer cells, we may need to adjust our viewpoint and should consider these compounds not as multi-action prodrugs but as prodrugs that effectively deliver CA4, rather than cisplatin, to the tumor.

## EXPERIMENTAL SECTION

**General Methods.** Oxoplatin,<sup>46</sup> 4-phenylbutyric anhydride, valproic anhydride, and octanoic anhydride were prepared by following the established procedures.<sup>47</sup> Combretastatin A4 (from Abosyn Chemical Inc., USA) and DCA anhydride (from Sigma-Aldrich, Germany) were commercially purchased.

**Characterization.** All complexes were characterized by <sup>1</sup>H-, <sup>13</sup>C-, and <sup>195</sup>Pt-NMR and ESI mass spectrometry and the high purity (>95%) was confirmed by HPLC measurements (see Figures S36–S44) and elemental analysis. The obtained data were consistent with the proposed structures.

All NMR data were recorded on a Bruker AVANCE III HD 500 MHz spectrometer. The data were processed using a MestreNova. <sup>1</sup>H and <sup>13</sup>C NMR chemical shifts were referenced with the individual solvent residual peaks of the respective NMR solvents. <sup>195</sup>Pt NMR chemical shifts were reported with respect to the chemical shift of the standard K<sub>2</sub>PtCl<sub>4</sub> in water at –1624 ppm. Electrospray ionization mass spectra (ESI-MS) were done using a Thermo Scientific triple quadrature mass spectrometer (Quantum Access) by the positive mode ESI. Elemental analyses were performed using a Thermo Scientific FLASH 2000 element analyzer. All compounds were characterized by HPLC on a Thermo Scientific UltiMate 3000 HPLC using one of the following methods.

**Purification by Preparative HPLC.** Compounds (3)–(9) were purified on a Thermo Scientific UltiMate 3000 preparative HPLC equipped with a RP-18 phase column (Phenomenex Luna, length 250 cm × internal diameter 21.2 mm, particle size 10 μM, and pore size 100 Å). Method settings: flow rate 15.0 mL/min, wavelength 220 nm (UV detector), water–ACN gradient (5 min 100% water to equilibrate, in 15 min from 0 to 100% ACN, 10 min 100% ACN), room temperature. Method A: LC XB-C18 column (Phenomenex Kinetex, length 250 mm, internal diameter 4.60 mm, particle size 5 μM, and pore size 100Å). Settings: flow rate 1.0 mL/min, wavelength 220 nm (UV detector), water–ACN gradient (5 min 100% water to equilibrate, in 15 min from 0 to 100% ACN, and 5 min 100% ACN), and room temperature. Used for compounds (2)–(7). Method B: LC XB-C18 column (Phenomenex Kinetex, length 100 mm, internal diameter 4.60 mm, particle size 2.6 μM, and pore size 100Å). Settings: flow rate 1.0 mL/min, wavelength 220 nm (UV detector), water–ACN gradient (1.84 min

100% water to equilibrate, in 5.84 min from 0 to 100% ACN, 2 min 100% ACN), and room temperature. Used for compounds (8)–(10).  
**Synthesis of Carbonate Compounds (2)–(7).**

- (i) 500.0 mg of CA4 (1) (1.581 mmol), 809.5 mg of DSC (3.161 mmol), and 183.4 mg of DMAP (1.502 mmol) were stirred at room temperature in 20 mL of DCM for 3 h and monitored by HPLC. Afterward, the solution was washed three times with 20 mL of distilled water and dried by addition of  $\text{Na}_2\text{SO}_4$ , filtered, and evaporated to dryness under reduced pressure at room temperature. The activated CA4 (CA4-DSC) was isolated as a fluffy white solid, yielding 90.3%. It was used without any further purification. HPLC purity was > 95%. The product was stored at  $-4^\circ\text{C}$ .
- (ii) 300.0 mg of CA4-DSC (0.656 mmol) and 175.3 mg of oxoplatin (0.525 mmol) were stirred at  $35^\circ\text{C}$  in 25 mL dimethylformamide (DMF) for 16 h. The reaction was monitored by platinum NMR. After the complete conversion to cisPt(CA4)(OH) (2), DMF was evaporated under reduced pressure at  $35^\circ\text{C}$ . The yellow residue was dissolved in 2 mL of MeOH, and 48 mL of diethyl ether was added to precipitate the pure product. After centrifugation, diethyl ether was decanted, the product was washed again twice with 10 mL of diethyl ether, and dried at room temperature under reduced pressure, yielding 84.8% of cisPt(CA4)(OH) (2) as a pure pale yellow solid. The product was stored at  $-4^\circ\text{C}$ .
- (iii) 80.0 mg of cisPt(CA4)(OH) (2) (0.118 mmol) and either CA4-DSC or the respective anhydrides (0.473 mmol) were stirred in 2 mL of DMF at room temperature for 24 h up to 5 days. The reaction was monitored by platinum NMR and HPLC. After the complete conversion, DMF was evaporated and the pure products (3)–(7) were obtained as a solid after purification by preparative HPLC. The products were stored at  $-4^\circ\text{C}$ .

**Synthesis of Carboxylate Compounds (8)–(10).**

- (iv) 200.0 mg of CA4 (0.634 mmol) was stirred with glutaric anhydride (0.951 mmol) and TEA (1.903 mmol) in 5 mL of DCM at room temperature for 2 h. The reaction was monitored by thin-layer chromatography (2% MeOH in DCM:  $R_f(\text{CA4}) = 0.5$ ,  $R_f(\text{CA4-glutaric}) = 0.17$ ). After the complete conversion, the compound was isolated by a separating funnel with DCM and water (adjusted with hydrochloric acid to pH 2). The organic phases were combined, dried over  $\text{Na}_2\text{SO}_4$ , filtered, and evaporated at room temperature. The desired compound was obtained as an oil, which was washed with hexane for 1 h. Hexane was decanted and the white solid residue was washed twice more with hexane. CA4-glu (8) was suspended in distilled water and dried by lyophilization overnight and a fluffy white solid was obtained, yielding 92.6%.
- (v) 200 mg of CA4-glu (0.465 mmol) was activated by the addition of EDC (0.558 mmol) and NHS (0.558 mmol) and stirred in 2 mL of DMF for 4 h at room temperature. The reaction was monitored by HPLC. After the complete conversion of CA4-glu to CA4-glu-DSC, DMF was evaporated, and the product was purified by preparative HPLC, yielding 91.2%.
- (vi) 95 mg of CA4-glu-DSC (0.180 mmol) was stirred with oxoplatin (0.144 mmol) in 15 mL of DMF for 16 h. The reaction was monitored by  $^{195}\text{Pt}$  NMR. After the complete conversion, DMF was evaporated and the product cisPt(CA4-glu)(OH) (9) was purified by preparative HPLC and dried by lyophilization. A pure white solid was obtained with a yield of 33.5%.
- (vii) 24 mg of cisPt(CA4-glu)(OH) (0.032 mmol) was dissolved in 3 mL of DMF and phenyl butyric anhydride (0.129 mmol) was added. The reaction was stirred for 16 h at room temperature. Afterward, the solvent was removed under reduced pressure. Methanol was added, and the final complex was purified by preparative HPLC and dried by lyophilization. A pure white solid (10) was gained, yielding 61%.

cisPt(CA4)(OH) (2)  $^1\text{H}$  NMR (500 MHz,  $\text{DMSO}-d_6$ ):  $\delta$  7.06 (m, 2H,  $-\text{CH}$ ), 6.99 (d,  $J = 8.4$  Hz, 1H,  $-\text{CH}$ ), 6.57 (s, 2H,  $-\text{CH}$ ), 6.47 (q,  $J = 12.3$  Hz, 2H,  $-\text{CH}$ ), 5.96 (m, 6H,  $-\text{NH}_3$ ), 3.75 (s, 3H,  $-\text{OCH}_3$ ),

3.65 (s, 3H,  $-\text{OCH}_3$ ), 3.61 (s, 6H,  $-\text{OCH}_3$ ).  $^{13}\text{C}$  NMR (126 MHz,  $\text{DMSO}-d_6$ ):  $\delta$  157.95, 153.04, 150.94, 141.69, 137.19, 132.47, 129.50, 129.43, 129.10, 126.20, 123.89, 112.86, 106.43, 60.53, 56.14, 56.09.  $^{195}\text{Pt}$  NMR (108 MHz,  $\text{DMSO}-d_6$ ):  $\delta$  1058.53. Elemental analysis for  $\text{C}_{19}\text{H}_{26}\text{Cl}_2\text{N}_2\text{O}_8\text{Pt}\cdot\text{H}_2\text{O}$  calcd/found: (C 32.86/32.98 H 4.06/3.98 N 4.03/3.83). MS-ESI (positive mode):  $m/z$   $[\text{M} + \text{H}]^+$  676.93,  $[\text{M} + \text{Na}]^+$  696.87.

cisPt(CA4)(PhB) (3)  $^1\text{H}$  NMR (500 MHz,  $\text{DMSO}-d_6$ ):  $\delta$  7.28 (t,  $J = 7.5$  Hz, 2H,  $-\text{CH}$ ), 7.19 (m, 3H,  $-\text{CH}$ ), 7.09 (d,  $J = 8.2$  Hz, 2H,  $-\text{CH}$ ), 7.01 (d,  $J = 8.2$  Hz, 1H,  $-\text{CH}$ ), 6.56 (s, 2H,  $-\text{CH}$ ), 6.47 (m, 2H,  $-\text{CH}$ ), 3.76 (s, 3H,  $-\text{OCH}_3$ ), 3.65 (s, 3H,  $-\text{OCH}_3$ ), 3.61 (s, 6H,  $-\text{OCH}_3$ ), 2.60 (t,  $J = 7.6$  Hz, 2H,  $-\text{CH}_2$ ), 2.25 (t,  $J = 7.4$  Hz, 2H,  $-\text{CH}_2$ ), 1.75 (p,  $J = 7.5$  Hz, 2H,  $-\text{CH}_2$ ).  $^{13}\text{C}$  NMR (126 MHz,  $\text{DMSO}-d_6$ ):  $\delta$  207.04, 180.80, 157.60, 153.05, 150.79, 142.42, 141.10, 137.20, 132.42, 129.57, 128.95, 128.70, 126.69, 126.17, 123.65, 112.99, 106.41, 60.54, 56.20, 56.09, 35.02, 32.02, 28.75.  $^{195}\text{Pt}$  NMR (108 MHz,  $\text{DMSO}-d_6$ ):  $\delta$  1233.89. Elemental analysis for  $\text{C}_{29}\text{H}_{36}\text{Cl}_2\text{N}_2\text{O}_9\text{Pt}$  calcd/found: (C 42.34/42.36 H 4.41/4.55 N 3.41/3.11). MS-ESI (positive mode):  $m/z$   $[\text{M} + \text{H}]^+$  822.95,  $[\text{M} + \text{NH}_4]^+$  839.74.

cisPt(CA4)(CA4) (4)  $^1\text{H}$  NMR (500 MHz,  $\text{DMSO}-d_6$ ):  $\delta$  7.10 (m, 4H  $-\text{CH}$ ), 7.03 (d,  $J = 8.4$  Hz, 2H  $-\text{CH}$ ), 6.56 (s, 4H  $-\text{CH}$ ), 6.47 (q, 4H,  $-\text{CH}$ ), 3.76 (s, 6H  $-\text{OCH}_3$ ), 3.65 (s, 6H  $-\text{OCH}_3$ ), 3.61 (s, 12H  $-\text{OCH}_3$ ).  $^{13}\text{C}$  NMR (126 MHz,  $\text{DMSO}-d_6$ ):  $\delta$  157.38, 153.06, 150.70, 141.00, 137.22, 132.40, 129.65, 129.60, 128.93, 126.75, 123.70, 113.02, 106.43, 60.53, 56.22, 56.09.  $^{195}\text{Pt}$  NMR (108 MHz,  $\text{DMSO}-d_6$ ):  $\delta$  1256.75. Elemental analysis for  $\text{C}_{38}\text{H}_{44}\text{Cl}_2\text{N}_2\text{O}_{14}\text{Pt}$  calcd/found: (C 44.80/44.29 H 4.35/4.40 N 2.75/2.48). MS-ESI (positive mode):  $m/z$   $[\text{M} + \text{Na}]^+$  1040.85.

cisPt(CA4)(DCA) (5)  $^1\text{H}$  NMR (500 MHz,  $\text{DMSO}-d_6$ ):  $\delta$  ppm 7.11 (m, 2H  $-\text{CH}$ ), 7.03 (d,  $J = 8.3$  Hz, 1H  $-\text{CH}$ ), 6.53 (s, 2H  $-\text{CH}$ ), 6.47 (q, 2H,  $-\text{CH}$ ), 3.76 (s, 6H  $-\text{OCH}_3$ ), 3.65 (s, 6H  $-\text{OCH}_3$ ), 3.61 (s, 12H  $-\text{OCH}_3$ ).  $^{13}\text{C}$  NMR (126 MHz,  $\text{DMSO}-d_6$ ):  $\delta$  ppm 170.87, 157.46, 153.06, 150.71, 140.98, 137.22, 132.40, 129.64, 129.60, 128.92, 126.79, 123.67, 113.02, 106.46, 65.60, 60.54, 56.22, 56.09.  $^{195}\text{Pt}$  NMR (108 MHz,  $\text{DMSO}-d_6$ ):  $\delta$  ppm 1230.24. Elemental analysis for  $\text{C}_{21}\text{H}_{26}\text{Cl}_4\text{N}_2\text{O}_9\text{Pt}$  calcd/found: (C 32.04/32.09 H 3.33/3.30 N 3.56/3.29). MS-ESI (positive mode):  $m/z$   $[\text{M} + \text{H}]^+$  786.74,  $[\text{M} + \text{NH}_4]^+$ , 803.39,  $[\text{M} + \text{Na}]^+$  808.72.

cisPt(CA4)(OCT) (6)  $^1\text{H}$  NMR (500 MHz,  $\text{DMSO}-d_6$ ):  $\delta$  ppm 7.08 (m, 2H  $-\text{CH}$ ), 7.01 (d,  $J = 8.3$  Hz, 1H  $-\text{CH}$ ), 6.56 (s, 2H  $-\text{CH}$ ), 6.48 (q, 4H,  $-\text{CH}$ ), 3.76 (s, 6H  $-\text{OCH}_3$ ), 3.65 (s, 6H  $-\text{OCH}_3$ ), 3.61 (s, 12H  $-\text{OCH}_3$ ), 2.24 (t,  $J = 7.5$  Hz, 2H  $-\text{CH}_2$ ), 1.46 (m, 2H  $-\text{CH}_2$ ), 1.25 (m, 8H  $-\text{CH}_2$ ), 0.87 (t,  $J = 6.8$  Hz, 3H  $-\text{CH}_3$ ).  $^{13}\text{C}$  NMR (126 MHz,  $\text{DMSO}-d_6$ ):  $\delta$  181.14, 157.59, 153.06, 150.80, 141.11, 137.21, 132.42, 129.58, 128.96, 126.66, 123.68, 112.99, 106.42, 60.53, 56.20, 56.09, 35.67, 31.66, 29.49, 29.02, 25.88, 22.56, 14.45.  $^{195}\text{Pt}$  NMR (108 MHz,  $\text{DMSO}-d_6$ ):  $\delta$  ppm 1235.96. Elemental analysis for  $\text{C}_{27}\text{H}_{40}\text{Cl}_2\text{N}_2\text{O}_9\text{Pt}$  calcd/found: (C 40.41/40.76 H 5.02/5.11 N 3.49/3.41). MS-ESI (positive mode):  $m/z$   $[\text{M} + \text{H}]^+$  802.70,  $[\text{M} + \text{Na}]^+$  824.96,  $[\text{M} + \text{K}]^+$  840.78.

cisPt(CA4)(VAL) (7)  $^1\text{H}$  NMR (500 MHz,  $\text{DMSO}-d_6$ ):  $\delta$  7.09 (m, 2H,  $-\text{CH}$ ), 7.02 (d,  $J = 8.5$  Hz, 1H,  $-\text{CH}$ ), 6.57 (s, 2H,  $-\text{CH}$ ), 6.48 (q,  $J = 10.5$  Hz, 2H,  $-\text{CH}$ ), 3.76 (s, 3H,  $-\text{OCH}_3$ ), 3.65 (s, 3H,  $-\text{OCH}_3$ ), 3.61 (s, 6H,  $-\text{OCH}_3$ ), 2.81 (s, 1H,  $-\text{CH}$ ), 1.38 (m, 8H  $-\text{CH}_2$ ), 0.84 (t, 6H,  $-\text{CH}_3$ ).  $^{13}\text{C}$  NMR (126 MHz,  $\text{DMSO}-d_6$ ):  $\delta$  184.41, 157.51, 153.04, 150.94, 141.69, 137.21, 132.42, 129.60, 129.59, 128.98, 126.60, 123.76, 112.98, 106.43, 60.53, 56.20, 56.09, 46.59, 42.57, 35.12, 34.60, 25.95, 20.47, 14.63.  $^{195}\text{Pt}$  NMR (108 MHz,  $\text{DMSO}-d_6$ ):  $\delta$  1240.19. Elemental analysis for  $\text{C}_{27}\text{H}_{40}\text{Cl}_2\text{N}_2\text{O}_9\text{Pt}\cdot\text{EtOH}$  calcd/found: (C 41.04/41.46 H 5.46/5.23 N 3.30/3.39). MS-ESI (positive mode):  $m/z$   $[\text{M} + \text{H}]^+$  802.84,  $[\text{M} + \text{Na}]^+$  824.96.

CA4-glu (8)  $^1\text{H}$  NMR (500 MHz,  $\text{DMSO}-d_6$ ):  $\delta$  7.15 (dd,  $J = 8.4$ , 2.1 Hz, 1H,  $-\text{CH}$ ), 7.06 (d,  $J = 8.5$ , 1H,  $-\text{CH}$ ), 6.99 (d,  $J = 2.1$  Hz, 1H,  $-\text{CH}$ ), 6.54 (s, 2H,  $-\text{CH}$ ), 6.50 (q, 2H,  $-\text{CH}$ ), 3.74 (s, 3H,  $-\text{OCH}_3$ ), 3.64 (s, 3H,  $-\text{OCH}_3$ ), 3.60 (s, 6H,  $-\text{OCH}_3$ ), 2.56 (t,  $J = 7.3$  Hz, 2H,  $-\text{CH}_2$ ), 2.32 (t,  $J = 7.4$  Hz, 2H,  $-\text{CH}_2$ ), 1.81 (p,  $J = 7.5$  Hz, 2H,  $-\text{CH}_2$ ).  $^{13}\text{C}$  NMR (126 MHz,  $\text{DMSO}-d_6$ ):  $\delta$  173.99, 170.74, 152.63, 149.99, 138.97, 136.78, 131.97, 129.52, 129.39, 128.27, 127.39, 122.67, 112.65, 105.89, 60.05, 55.85, 55.55, 32.38, 32.32, 20.00. Elemental analysis for  $\text{C}_{23}\text{H}_{26}\text{O}_8$  calcd/found: (C 64.18/63.98 H 6.09/6.20). MS-ESI

(positive mode):  $m/z$   $[M + H]^+$  431.10,  $[M + NH_4]^+$  448.11,  $[M + Na]^+$  453.08,  $[M + K]^+$  469.18.

cisPt(CA4-glu)(OH) (9)  $^1H$  NMR (500 MHz, DMSO- $d_6$ ):  $\delta$  7.14 (dd, 1H, -CH), 7.06 (d, 1H, -CH), 6.98 (dd, 1H, -CH), 6.54 (s, 2H, -CH), 6.50 (q, 2H, -CH), 5.93 (m, 6H, -NH<sub>3</sub>), 3.75 (s, 3H, -OCH<sub>3</sub>), 3.64 (s, 3H, -OCH<sub>3</sub>), 3.60 (s, 6H, -OCH<sub>3</sub>), 2.56 (t, 2H, -CH<sub>2</sub>), 2.27 (t, 2H, -CH<sub>2</sub>), 1.77 (p, 2H, -CH<sub>2</sub>).  $^{13}C$  NMR (126 MHz, DMSO- $d_6$ ):  $\delta$  180.64, 171.58, 153.08, 150.53, 139.53, 137.22, 132.44, 129.96, 129.83, 128.78, 127.75, 123.18, 113.13, 106.37, 60.56, 56.40, 56.04, 35.66, 33.10, 21.58.  $^{195}Pt$  NMR (108 MHz, DMSO- $d_6$ ):  $\delta$  1037.72. Elemental analysis for C<sub>23</sub>H<sub>32</sub>Cl<sub>2</sub>N<sub>2</sub>O<sub>9</sub>Pt calcd/found: (C 37.01/37.35 H 4.32/4.02 N 3.75/3.32). MS-ESI (positive mode):  $m/z$   $[M + H]^+$  746.19,  $[M + Na]^+$  768.10,  $[M + K]^+$  784.06.

cisPt(CA4-glu)(PhB) (10)  $^1H$  NMR (500 MHz, DMSO- $d_6$ ):  $\delta$  7.33–7.03 (m, 8H), 6.98 (d,  $J$  = 2.2 Hz, 1H), 6.67–6.40 (m, 9H), 3.75 (d,  $J$  = 5.7 Hz, 3H), 3.64 (d,  $J$  = 1.7 Hz, 3H), 3.61 (d,  $J$  = 3.2 Hz, 6H), 2.59 (dt,  $J$  = 9.4,  $J$  = 7.4 Hz, 4H), 2.35 (t,  $J$  = 7.3 Hz, 2H), 2.23 (t,  $J$  = 7.3 Hz, 2H), 1.77 (dt,  $J$  = 15.0, 7.4 Hz, 4H).  $^{13}C$  NMR (126 MHz, DMSO- $d_6$ ):  $\delta$  181.10, 180.49, 171.48, 153.08, 150.51, 142.47, 139.50, 137.22, 132.44, 129.97, 129.85, 128.95, 128.77, 128.69, 127.78, 126.15, 123.16, 113.14, 106.37, 60.56, 56.40, 56.04, 48.40, 35.54, 34.91, 32.92, 27.99, 21.35.  $^{195}Pt$  NMR (108 MHz, DMSO- $d_6$ ):  $\delta$  1218.45. Elemental analysis for C<sub>33</sub>H<sub>42</sub>Cl<sub>2</sub>N<sub>2</sub>O<sub>10</sub>Pt calcd/found: (C 44.40/44.18 H 4.74/5.08 N 3.14/3.18). MS-ESI (positive mode):  $m/z$   $[M + H]^+$  892.96,  $[M + Na]^+$  914.79,  $[M + K]^+$  731.06.

**Stability Studies by RP-HPLC.** HPLC studies were performed on a Thermo Scientific UltiMate 3000 HPLC. Preparation for ACN/medium and buffer/medium: 500  $\mu$ L of a stock solution, containing the respective compound in acetonitrile (1.2  $\mu$ M), was prepared and 500  $\mu$ L of either RPMI cell culture medium (without any supplements) or phosphate buffer (50 mM, pH 7.0) was added. Preparation for DMSO/medium: 10  $\mu$ L of DMSO was added to compounds, and after they were solubilized, 990  $\mu$ L of 1640 RPMI were added to achieve a final concentration of 1% DMSO. After appropriate mixing, the samples were filtered through a PreTech syringe Nylon filter (13 mm, 0.22  $\mu$ m), stored at 37 °C, and injected several times until the decomposition was completed, and the test complexes were hydrolyzed more than 50%. Method C: LC XB-C18 column (Phenomenex Kinetex, length 250 mm, internal diameter 4.60 mm, particle size 5  $\mu$ M, and pore size 100Å). Settings: flow rate 1.0 mL/min, wavelength 220 nm (UV detector), water–ACN gradient (2 min 100% water to equilibrate, in 15 min from 0 to 100% ACN, 3 min 100% ACN), and autosampler temperature 37 °C. Used for compounds (2)–(5), (7). Method D: LC XB-C18 column (Phenomenex Kinetex, length 100 mm, internal diameter 4.60 mm, particle size 2.6  $\mu$ M, and pore size 100Å). Settings: flow rate 1.0 mL/min, wavelength 220 nm (UV detector), water–ACN gradient (1.84 min 100% water to equilibrate, in 5.84 min from 0 to 100% ACN, 2 min 100% ACN), and autosampler temperature 37 °C. Used for compounds (6) and (8)–(10).

**Reduction Studies by RP-HPLC and  $^1H$  NMR.** RP-HPLC: 500  $\mu$ L of a stock solution, containing the respective compound in acetonitrile (1.2  $\mu$ M), was prepared and 500  $\mu$ L of an ascorbic acid solution (12  $\mu$ M) of phosphate buffer (50 mM, pH 7.0) was added. After appropriate mixing, the samples were filtered through a PreTech syringe Nylon filter (13 mm, 0.22  $\mu$ m), stored at 37 °C, and injected several times until the reduction was completed, and the test complexes were fully reduced. Method C: used for compounds (2)–(5), (7). Method D: used for compounds (6), (8)–(10).  $^1H$  NMR: 1 mg of the respective complexes cisPt(CA4)(OH) and cisPt(CA4-glu)(OH) was dissolved in 750  $\mu$ L of DMSO- $d_6$  and  $^1H$  NMR were recorded. Afterward, 10 equiv of ascorbic acid was added to each same sample tube, mixed carefully to ensure that all reagents are completely dissolved, and the reduction of each complex was monitored up to 24 h (every 5 min for cisPt(CA4)(OH) and every hour for cisPt(CA4-glu)(OH)).

**Cell Culture.** Maintenance: HT-29 human colon carcinoma cells, MDA-MB-231 human breast cancer cells, MCF-7 human breast carcinoma cells, and SK-HEP-1 human liver adenocarcinoma cells were maintained in Dulbecco's modified Eagle's medium (4.5 g/L (D)-glucose, L-glutamine, and pyruvate) from Life Technologies, which was

supplemented with gentamycin (50 mg/L) and fetal bovine serum superior, standardized (Biochrom GmbH, Berlin) (10% v/v), and were passaged once a week. RC-124 human kidney cells were maintained in McCoy's 5A (modified, with L-glutamine) medium (Life Technologies), which was supplemented with gentamycin (50 mg/L) and fetal bovine serum superior, standardized (Biochrom GmbH, Berlin) (10% v/v), and also passaged once a week. For experiments with RC-124 cells, microtiter plates had been pretreated in the following way: 30 mL of a sterilized gelatin solution [1.5% (m/v)] was added to each well of flat-bottom 96-well plates, the plates were covered with their lids, incubated for 1 h at 37 °C, the excess solution was removed, and the wells were washed once with phosphate-buffered saline (PBS) (140 mM NaCl, 3 mM KCl, 10 mM Na<sub>2</sub>HPO<sub>4</sub>, 1.8 mM KH<sub>2</sub>PO<sub>4</sub>; pH 7.4), and the new cell culture medium was added. HT-29, MCF-7, SK-HEP-1, and RC-124 cells were obtained from Cell Line Service (CLS, Eppenheim, Germany) and MDA-MB-231 cells from the Helmholtz Institute for Infection Research (HZI, Braunschweig, Germany).

A375 human malignant melanoma cells, A2780 human ovarian carcinoma cells, and A2780cis cisplatin-resistant ovarian carcinoma cells were cultured in RPMI 1640 (no glutamine) supplemented with heat-inactivated fetal bovine serum (South American origin) (10% v/v), gentamycin sulfate solution (1% v/v), and L-glutamine solution 200 nM (1% v/v). PC9 human non-small cell lung carcinoma cells were maintained in DMEM (high glucose, no glutamine/sodium pyruvate) supplemented with L-glutamine solution (200 nM) (1% v/v), 10% (v/v) heat-inactivated fetal bovine serum (South American origin, European grade), and 1% (v/v) penicillin–streptomycin solution (containing penicillin G sodium salt: 10,000 units/mL and streptomycin sulfate: 10 mg/mL) and were passaged twice a week. Once a week, a solution of cisplatin in RPMI medium (end concentration: 1  $\mu$ M) was added to A2780cis cells to maintain the resistance. All reagents were purchased at Biological Industries. A375, PC9, A2780, and A2780cis cells were obtained from the American Type Culture Collection (ATCC, Rockville, MD).

**Antiproliferative Assay in Tumorigenic and Non-tumorigenic Cells.** The antiproliferative effects were determined according to a recently used method with minor modifications.<sup>15,48</sup> In short: SK-HEP-1 cells, HT-29 cells, MDA-MB-231 cells, MCF-7 cells, or RC-124 cells were transferred into each well of a flat-bottom 96-well microtiter plate (note: for RC-124, pretreated plates were used, see above) and incubated at 37 °C/5% CO<sub>2</sub> for either 72 h. Stock solutions of the compounds in cell culture medium (cisplatin as reference) or DMSO (compounds (1)–(9)) were freshly prepared and diluted with the respective cell culture medium to graded concentrations (a final concentration of DMSO: 0.1% v/v). After 72 h of exposure, the cell biomass was determined by crystal violet (Sigma-Aldrich) staining at a wavelength of 590 nm.

A357 melanoma cells (4000 cells/well), A2780 ovarian carcinoma cells (5000 cells/well), A2780cis cisplatin-resistant ovarian carcinoma cells (7000 cells/well), and PC9 small lung cell carcinoma cells (4000 cells/well) were seeded in flat-bottom 96-well plates and incubated at 37 °C/5% CO<sub>2</sub> for 24 h. Stock solutions of the compounds in DMSO (compounds (1)–(9)) or cell culture medium (cisplatin as reference) were freshly prepared and diluted with the respective cell culture medium to graded concentrations (final concentration of DMSO: 0.1% v/v). After 72 h of exposure, the cell biomass was determined by 3-(4,5-dimethylthiazol-2-yl)-2,5-diphenyl tetrazolium bromide (MTT) (Sigma-Aldrich) staining, and the absorptions were calculated as the delta of two measurements of the same well at wavelengths 570 and 690 nm.

The IC<sub>50</sub> values were determined as the concentration that caused 50% inhibition of cell proliferation compared to an untreated control. The results were calculated as the mean values of three independent experiments.

**Protein Binding Studies with FCS Proteins.** Protein binding of the platinum complexes was studied using a modified precipitation assay reported earlier by Ma et al.<sup>49</sup> FCS was chosen as the representative protein since it is used in all the cell culture experiments. Cell culture medium (DMEM) was reconstituted with 10% FCS. The CA4–platinum complexes were dissolved in DMSO to prepare a stock

solution (10 mM), and cisplatin was dissolved in Millipore water and diluted to the same concentration. Each stock solution was added to the reconstituted medium such that the final concentration was 50  $\mu\text{M}$  in a total volume of 5 mL. They were incubated at 37 °C for different time points (0, 2, 4, 8, and 24 h). Untreated reconstituted media was treated identically as the other samples and used as the matrix for calibration. Aliquots (500  $\mu\text{L}$ ) of each sample were treated with ice-cold ethanol (1 mL) and stored at -25 °C for 3 h. Thereafter, the samples were centrifuged (964 g at 4 °C for 30 min). The supernatant was isolated and stored at -25 °C for the final measurements. An aliquot (500  $\mu\text{L}$ ) of each sample was treated with 10% nitric acid (4.5 mL) and the samples were further diluted using Millipore water. For calibration, a standard solution of platinum (1.0 ppm Pt standard solution procured from Sigma-Aldrich, ICP grade) was added in graded concentrations to the untreated sample. The platinum in the samples was measured using ICP optical emission spectroscopy (Agilent Technologies ICP-OES, 5110) equipped with a SPS4 autosampler. The values reported are the average of three independent measurements.

**Cellular Uptake Studies in MDA-MB-231 Cancer Cells.** Cellular accumulations of studied complexes were determined in highly invasive human breast carcinoma cells MDA-MB-231. In these experiments,  $1 \times 10^6$  MDA-MB-231 cells were seeded on 100 mm Petri dishes. After overnight pre-incubation in a drug-free medium at 37 °C in a 5%  $\text{CO}_2$  humidified atmosphere, the cells were treated with platinum compounds and allowed a further 5 h of drug exposure under similar conditions. After treatment, the cells were extensively washed with PBS (37 °C), detached by using 0.25% trypsin, washed twice with ice-cold PBS, and counted. The cell pellets were stored at -70 °C and digested using a microwave acid (HCl) digestion system (CEM Mars). The quantity of metal taken up by the cells was determined by ICP-MS using Agilent 7500 (Agilent, Japan). All experiments were carried out in triplicate.

**Analysis of Tubulin Polymerization in MDA-MB-231 Cells.** MDA-MB-231 cells were seeded in 60 mm Petri dishes ( $3 \times 10^5$  cells/well) and grown overnight. Following the 8 h treatment at the indicated concentrations, the cells were harvested by trypsinization, washed, and pelleted. Subsequently, the cells were fixed in 1 mL of microtubule-stabilizing buffer (80 mM pipes, pH 6.8, 5 mM ethylenediaminetetraacetic acid, 1 mM  $\text{MgCl}_2$ , 0.5% Triton X-100, and 0.5% glutaraldehyde) for 10 min at room temperature. Glutaraldehyde was then quenched with 0.7 mL of  $\text{NaBH}_4$  in PBS. The cells were pelleted and resuspended in antibody dilution solution (PBS, pH 7.4, 2% BSA 0.2% Triton X-100, 0.1%  $\text{NaN}_3$ ). After a 3 h incubation with anti- $\alpha$ -tubulin-FITC antibody (mouse monoclonal; Sigma-Aldrich, Prague; 1:250 dilution), the cells were analyzed by a FACSVerser flow cytometer (Becton Dickinson, Germany) and data analyzed using ModFit LT 4.1 software (Verity Software House).

**Tubulin Polymerization Inhibition in a Cell-Free Medium.** Fluorescence-based tubulin polymerization assay kit (porcine tubulin; Cytoskeleton, Inc.) was used to analyze the influence of the tested compounds on tubulin polymerization *in vitro*. The experiment was performed following the manufacturer's protocol. Briefly, 2 mg  $\text{mL}^{-1}$  tubulin in tubulin glycerol buffer (80 mM pipes; 2 mM  $\text{MgCl}_2$  0.5 mM EGTA, pH 6.9; 1 mM GTP; 15% glycerol; and 10  $\mu\text{M}$  fluorescent reporter) was polymerized in the absence or presence of the tested compounds (1, 5, and 10  $\mu\text{M}$ ) at 37 °C for 40 min. Fluorescence signal (EX 350 nm/EM 450 nm) was read once per minute using a Varian Cary Eclipse spectrofluorophotometer.

**Quantification of Platinum Bound to DNA Isolated from MDA-MB-231 Cells.** MDA-MB-231 cells were treated with the tested compounds at a concentration of 0.1 and 1.0  $\mu\text{M}$  for 5 h or 0.01  $\mu\text{M}$  for 24 h at 37 °C. The cell pellets were stored at -70 °C and then lysed in DNAzol (DNAzol, MRC) supplemented with RNase A (100  $\mu\text{g mL}^{-1}$ ). Genomic DNA was precipitated from the lysate by 100% ethanol, washed twice with 75% ethanol, and resuspended in 8 mM NaOH. The DNA content in each sample was determined by UV spectrophotometry. To avoid the affection of high DNA concentration on the detection of platinum in the samples, the DNA samples were digested in the presence of 30% hydrochloric acid (Suprapur, Merck Millipore).

The amount of platinum bound to nucleic acids was quantified by ICP-MS. All measurements were done in triplicate.

To determine the amount of platinum associated with DNA, the cells were prepared and treated similarly to cellular uptake studies. Following the treatment, the cells were detached with 0.25% trypsin and extensively washed, and the pellets were lysed using DNAzol (DNAzol genomic DNA isolation reagent, MRC) supplemented with RNase A (100  $\mu\text{g mL}^{-1}$ ). DNA was precipitated with ethanol, washed with 70% ethanol, and resolved in  $\text{H}_2\text{O}$ . DNA amount was determined spectrophotometrically and Pt content was measured with ICP-MS. The experiment was performed in triplicate.

**Antiproliferative Activity of Pt-CA4 Compounds in CHO-K1 and MMC-2 Cells.** Chinese hamster ovary CHO-K1 cell line (wild type) and its mutant cell line MMC-2 were kindly supplied by Dr. M. Pírsel (Cancer Research Institute, Slovak Academy of Sciences, Bratislava, Slovakia). The CHO-K1 and MMC-2 cells were grown in Dulbecco's modified Eagle's medium (DMEM, high glucose 4.5 g  $\text{L}^{-1}$ , PAA, Pasching, Austria) supplemented with gentamycin (50 mg  $\text{mL}^{-1}$ , Serva) and 10% heat-inactivated fetal bovine serum (PAA, Pasching, Austria). The cells were cultured in a humidified incubator at 37 °C in a 5%  $\text{CO}_2$  atmosphere and subcultured two to three times a week with an appropriate plating density. The cells were seeded in 96-well plates at a density of  $3 \times 10^5$  cells/well in 100  $\mu\text{L}$  medium. Following overnight incubation, the cells were treated with a series of concentrations of the investigated compounds in a final volume of 200  $\mu\text{L}$  for 72 h. At the end of the treatment, 20  $\mu\text{L}$  of the tetrazolium compound MTT solution (Calbiochem, Darmstadt, Germany) (1.25 mg  $\text{mL}^{-1}$  in PBS) was added. After another 2–4 h, the medium was removed, and the resulting formazan product was dissolved in 100  $\mu\text{L}$  DMSO. Absorbance was measured at 570 nm (ref. 620 nm) with an absorbance reader (SUNRISE TECAN, 1086 SCHOELLER). The  $\text{IC}_{50}$  values were determined as the drug concentration corresponding to 50% inhibition of the control signal.

**Microtubule Imaging.** MDA-MB-231 cells were grown on coverslips in six-well plates and treated with 1  $\mu\text{M}$  compounds (20  $\mu\text{M}$  in the case of oxoplatin) for 2 h. The cells were washed with PBS, fixed with 4% *p*-formaldehyde, and processed for immunostaining: permeabilization with 0.1% Tween-20 in PBS (PBST), blocking with 10% normal donkey serum in PBST, incubation with primary antibody (anti- $\beta$  I tubulin antibody; Abcam ab179511; 1:500) for 2 h, washed, incubated with secondary antibody (donkey anti-rabbit IgG Alexa Fluor 647; Abcam ab150075; 1:200) for 1 h, washed, and mounted with ProLong Diamond antifade with DAPI. The images were obtained with the laser-scanning microscope Leica TCS SP8 SMD (Leica Microsystems BmbH, Wetzlar, Germany).

**Cell Cycle Analysis.** MDA-MB-231 cells were seeded in six-well plates ( $6 \times 10^5$  cells/well), and following an overnight incubation, they were treated with tested compounds at concentrations corresponding to  $\text{IC}_{50}$  values (obtained with the MTT assay after a 72 h treatment). After a 24 h treatment, the cells were washed, detached with trypsin, washed twice with PBS, pelleted by centrifugation, and resuspended in 70% ethanol. Following a 1 h fixation, the cells were washed with PBS (2 $\times$ ) and stained with propidium iodide (50  $\mu\text{g mL}^{-1}$  in Vindel's solution—10 mM Tris-Cl (pH = 8.0), 10 mM NaCl, 0.1% Triton X-100, 100  $\mu\text{g mL}^{-1}$  RNase A) for 30 min at 37 °C. Cell cycle profiles were obtained with an FACSVerser flow cytometer (Becton Dickinson, Germany), and the data were analyzed with the ModFit LT 4.1 (Verity Software House). The experiment was performed three times.

**In Vivo Antitumor Activity in C57BL Lewis Lung Cell Carcinoma Mice.** In vivo anticancer activity toward LLC. All studies involving animal testing were carried out in accordance with ethical guidelines for animal research acknowledging the European Directive 2010/63/UE as to the animal welfare and protection and the related codes of practice (approval 640/2016-PR). The mice were purchased from Charles River, housed in steel cages under controlled environmental conditions (constant temperature, humidity, and 12 h dark/light cycle), and alimented with commercial standard feed and tap water ad libitum. The LLC cell line was purchased from ECACC, United Kingdom. The LLC cell line was maintained in DMEM (Euroclone) supplemented with 10% heat inactivated fetal bovine serum (Euroclone), 10 mM  $\text{L}^{-1}$

glutamine, 100 U mL<sup>-1</sup> penicillin, and 100 µg/mL streptomycin in a 5% CO<sub>2</sub> air incubator at 37 °C. The LLC was implanted intramuscularly (i.m.) as a 2 × 10<sup>6</sup> cell inoculum into the right hind leg of 8 week-old male C57BL mice (24 ± 3 g body weight). After 7 days from tumor implantation (visible tumors), mice were randomly divided into eight groups (five animals per group) and subjected to daily i.p. administration. Control mice received the vehicle [0.5% DMSO (v/v) and 99.5% of a saline solution (v/v)], whereas treated groups received daily doses of animals received daily oral gavage of 20 mg kg<sup>-1</sup> of Pt(CA4)(PhB), Pt(CA4)(OH), or cisPt(CA4-glu)(OH), daily i.p. of 3 mg kg<sup>-1</sup> of cisplatin, 20 mg kg<sup>-1</sup> of CA4 or PhB, and a combination of 3 mg kg<sup>-1</sup> of cisplatin, CA4, and PhB. At day 15, animals were sacrificed, the legs were amputated at the proximal end of the femur, and the inhibition of tumor growth was determined from the difference in the weights of the tumor-bearing leg and the healthy leg of the animals, expressed as a percentage referenced to the control animals. Body weight was measured at day 0 and from day 7 onward every 2 days and was taken as a parameter for systemic toxicity. All presented values are the means ± SD of no less than three measurements.

## ■ ASSOCIATED CONTENT

### Supporting Information

The Supporting Information is available free of charge at <https://pubs.acs.org/doi/10.1021/acs.jmedchem.1c00706>.

NMR and ESIMS spectra of the compounds as well as the HPLC chromatograms of all compounds (PDF)

Molecular formula strings of all the tested compounds (CSV)

## ■ AUTHOR INFORMATION

### Corresponding Authors

**Ingo Ott** – Institute of Medicinal and Pharmaceutical Chemistry, Technische Universität Braunschweig, 38106 Braunschweig, Germany; Email: [ingooott@tu-braunschweig.de](mailto:ingooott@tu-braunschweig.de)

**Valentina Gandin** – Dipartimento di Scienze del Farmaco, Università di Padova, 35131 Padova, Italy; Email: [valentina.gandin@unipd.it](mailto:valentina.gandin@unipd.it)

**Viktor Brabec** – Institute of Biophysics, Czech Academy of Sciences, 61265 Brno, Czech Republic; Department of Biophysics, Faculty of Science, Palacky University in Olomouc, 78371 Olomouc, Czech Republic; [orcid.org/0000-0002-8233-1393](https://orcid.org/0000-0002-8233-1393); Email: [brabec@ibp.cz](mailto:brabec@ibp.cz)

**Dan Gibson** – Institute for Drug Research, School of Pharmacy, The Hebrew University, 91120 Jerusalem, Israel; [orcid.org/0000-0002-1631-4018](https://orcid.org/0000-0002-1631-4018); Email: [dang@ekmd.huji.ac.il](mailto:dang@ekmd.huji.ac.il)

### Authors

**Claudia Schmidt** – Institute for Drug Research, School of Pharmacy, The Hebrew University, 91120 Jerusalem, Israel

**Tomer Babu** – Institute for Drug Research, School of Pharmacy, The Hebrew University, 91120 Jerusalem, Israel

**Hana Kostrhunova** – Institute of Biophysics, Czech Academy of Sciences, 61265 Brno, Czech Republic

**Annika Timm** – Institute of Medicinal and Pharmaceutical Chemistry, Technische Universität Braunschweig, 38106 Braunschweig, Germany

**Uttara Basu** – Institute of Medicinal and Pharmaceutical Chemistry, Technische Universität Braunschweig, 38106 Braunschweig, Germany

Complete contact information is available at:

<https://pubs.acs.org/doi/10.1021/acs.jmedchem.1c00706>

## Author Contributions

#C.S. and T.B. contributed equally to this work.

## Notes

The authors declare no competing financial interest.

## ■ ACKNOWLEDGMENTS

D.G. would like to acknowledge the support of the Israel Science Foundation (grant 1002/18). This research was also funded by the ICA-USA board member Bruce Youngman (D.G.). H.K. and V.B. acknowledge the support of the Czech Science Foundation (grant 21-27514S). We would like to acknowledge Dr. Gourab Dey of Prof. Galia Blum's research group at the Hebrew University of Jerusalem for helping with MS measurement and Petra Lippmann from I.O.'s lab at the Technische University of Braunschweig for supporting us with the crystal violet assay.

## ■ REFERENCES

- (1) Blomstrand, H.; Scheibling, U.; Bratthäll, C.; Green, H.; Elander, N. O. Real World Evidence on Gemcitabine and Nab-Paclitaxel Combination Chemotherapy in Advanced Pancreatic Cancer. *BMC Canc.* **2019**, *19*, 40.
- (2) Furugen, M.; Sekine, I.; Tsuta, K.; Horinouchi, H.; Nokihara, H.; Yamamoto, N.; Kubota, K.; Tamura, T. Combination Chemotherapy with Carboplatin and Paclitaxel for Advanced Thymic Cancer. *Jpn. J. Clin. Oncol.* **2011**, *41*, 1013–1016.
- (3) Dasari, S.; Bernard Tchounwou, P. Cisplatin in Cancer Therapy: Molecular Mechanisms of Action. *Eur. J. Pharmacol.* **2014**, *740*, 364–378.
- (4) Harmers, F. P.; Gispén, W. H.; Neijt, J. P. Neurotoxic Side-Effects of Cisplatin. *Eur. J. Canc.* **1991**, *27*, 372–376.
- (5) Pabla, N.; Dong, Z. Cisplatin Nephrotoxicity: Mechanisms and Renoprotective Strategies. *Kidney Int.* **2008**, *73*, 994–1007.
- (6) Galluzzi, L.; Senovilla, L.; Vitale, I.; Michels, J.; Martins, I.; Kepp, O.; Castedo, M.; Kroemer, G. Molecular Mechanisms of Cisplatin Resistance. *Oncogene* **2012**, *31*, 1869–1883.
- (7) Rose, P. G.; Blessing, J. A.; Gershenson, D. M.; McGehee, R. Paclitaxel and Cisplatin as First-Line Therapy in Recurrent or Advanced Squamous Cell Carcinoma of the Cervix: A Gynecologic Oncology Group Study. *J. Clin. Oncol.* **1999**, *17*, 2676.
- (8) Yang, Y.-F.; Wang, G.-Y.; He, J.-L.; Wu, F.-P.; Zhang, Y.-N. Overall Survival of Patients with KRAS Wild-Type Tumor Treated with FOLFOX/FOLFIRI +/- Cetuximab as the First-Line Treatment for Metastatic Colorectal Cancer: A Meta-Analysis. *Medicine* **2017**, *96*, No. e6335.
- (9) Papadatos-Pastos, D.; Thillai, K.; Rabbie, R.; Ross, P.; Sarker, D. FOLFIRINOX - A New Paradigm in the Treatment of Pancreatic Cancer. *Expert Rev. Anticancer Ther.* **2014**, *14*, 1115–1125.
- (10) Wexselblatt, E.; Gibson, D. What Do We Know About the Reduction of Pt(IV) Pro-Drugs? *J. Inorg. Biochem.* **2012**, *117*, 220–229.
- (11) Gibson, D. Multi-action Pt(IV) Anticancer Agents; Do We Understand How They Work? *J. Inorg. Biochem.* **2019**, *191*, 77–84.
- (12) Venkatesh, V.; Sadler, P. J. Platinum(IV) Prodrugs. *Met. Ions Life Sci.* **2018**, *18*, 69.
- (13) Kenny, R. G.; Marmion, C. J. Toward Multi-Targeted Platinum and Ruthenium Drugs-A New Paradigm in Cancer Drug Treatment Regimens? *Chem. Rev.* **2019**, *119*, 1058–1137.
- (14) Raveendran, R.; Braude, J. P.; Wexselblatt, E.; Novohradsky, V.; Stuchlikova, O.; Brabec, V.; Gandin, V.; Gibson, D. Pt(IV) Derivatives of Cisplatin and Oxaliplatin with Phenylbutyrate Axial Ligands are Potent Cytotoxic Agents that Act by Several Mechanisms of Action. *Chem. Sci.* **2016**, *7*, 2381–2391.
- (15) Babu, T.; Sarkar, A.; Karmakar, S.; Schmidt, C.; Gibson, D. Multi-action Pt(IV) Carbamate Complexes Can Codeliver Pt(II) Drugs and Amine Containing Bioactive Molecules. *Inorg. Chem.* **2020**, *59*, 5182–5193.
- (16) Petruzzella, E.; Sirota, R.; Solazzo, I.; Gandin, V.; Gibson, D. Triple Action Pt(IV) Derivatives of Cisplatin: a New Class of Potent

Anticancer Agents that Overcome Resistance. *Chem. Sci.* **2018**, *9*, 4299–4307.

(17) Mikula-Pietrasik, J.; Witucka, A.; Pakula, M.; Uruski, P.; Begier-Krasinska, B.; Niklas, A.; Tykarski, A.; Ksiazek, K. Comprehensive Review on How Platinum- and Taxane-Based Chemotherapy of Ovarian Cancer Affects Biology of Normal Cells. *Cell. Mol. Life Sci.* **2019**, *76*, 681–697.

(18) Pettit, G. R.; Singh, S. B.; Hamel, E.; Lin, C. M.; Alberts, D. S.; Garcia-Kendal, D. Antineoplastic Agents .145. Isolation and Structure of the Strong Cell-Growth and Tubulin Inhibitor Combretastatin-A-4. *Experientia* **1989**, *45*, 209–211.

(19) McGown, A. T.; Fox, B. W. Structural and Biochemical Comparison of the Anti-Mitotic Agents Colchicine, combretastatin A4 and Amphetamine. *Anticancer Drug Des.* **1989**, *3*, 249–254.

(20) Lin, C. M.; Ho, H. H.; Pettit, G. R.; Hamel, E. Antimitotic Natural Products Combretastatin A-4 and Combretastatin A-2: Studies on the Mechanism of their Inhibition of the Binding of Colchicine to Tubulin. *Biochemistry* **1989**, *28*, 6984–6991.

(21) Ferrari, S. M.; Elia, G.; Ragusa, F.; Ruffilli, I.; La Motta, C.; Paparo, S. R.; Patrizio, A.; Vita, R.; Benvenega, S.; Materazzi, G.; Fallahi, P.; Antonelli, A. Novel Treatments for Anaplastic Thyroid Carcinoma. *Gland Surg.* **2020**, *9*, S28–S42.

(22) Yempala, T.; Babu, T.; Karmakar, S.; Nemirovski, A.; Ishan, M.; Gandin, V.; Gibson, D. Expanding the Arsenal of Pt(IV) Anticancer Agents: Multi-action Pt(IV) Anticancer Agents with Bioactive Ligands Possessing a Hydroxy Functional Group. *Angew. Chem., Int. Ed. Engl.* **2019**, *58*, 18218–18223.

(23) Huang, X.; Huang, R.; Gou, S.; Wang, Z.; Liao, Z.; Wang, H. Combretastatin A-4 Analogue: A Dual-Targeting and Tubulin Inhibitor Containing Antitumor Pt(IV) Moiety with a Unique Mode of Action. *Bioconjugate Chem.* **2016**, *27*, 2132–2148.

(24) Li, L.; Huang, X.; Huang, R.; Gou, S.; Wang, Z.; Wang, H. Pt(IV) Prodrugs Containing Microtubule Inhibitors Displayed Potent Antitumor Activity and Ability to Overcome Cisplatin Resistance. *Eur. J. Med. Chem.* **2018**, *156*, 666–679.

(25) Huang, X.; Wang, M.; Wang, C. G.; Hu, W. W.; You, Q. H.; Yang, Y.; Yu, C. H.; Liao, Z. X.; Gou, S. H.; Wang, H. S. Dual-targeting Antitumor Conjugates Derived from Platinum(IV) Prodrugs and Microtubule Inhibitor CA-4 Significantly Exhibited Potent Ability to Overcome Cisplatin Resistance. *Bioorg. Chem.* **2019**, *92*, 103236.

(26) Novohradsky, V.; Zerkankova, L.; Stepankova, J.; Vrana, O.; Raveendran, R.; Gibson, D.; Kasparkova, J.; Brabec, V. New Insights Into the Molecular and Epigenetic Effects of Antitumor Pt(IV)-Valproic Acid Conjugates in Human Ovarian Cancer Cells. *Biochem. Pharmacol.* **2015**, *95*, 133–144.

(27) Dhar, S.; Lippard, S. J. Mitaplatin, a Potent Fusion of Cisplatin and the Orphan Drug Dichloroacetate. *Proc. Natl. Acad. Sci. U.S.A.* **2009**, *106*, 22199–22204.

(28) Novohradsky, V.; Zanellato, I.; Marzano, C.; Pracharova, J.; Kasparkova, J.; Gibson, D.; Gandin, V.; Osella, D.; Brabec, V. Epigenetic and Antitumor Effects of Platinum (IV)-Octanoato Conjugates. *Sci. Rep.* **2017**, *7*, 3751.

(29) Tron, G. C.; Piralì, T.; Sorba, G.; Pagliai, F.; Busacca, S.; Genazzani, A. A. Medicinal Chemistry of Combretastatin A4: Present and Future Directions. *J. Med. Chem.* **2006**, *49*, 3033–3044.

(30) Mostoufi, A.; Baghcoli, R.; Fereidoonzhad, M. Synthesis, Cytotoxicity, Apoptosis and Molecular Docking Studies of Novel Phenylbutyrate Derivatives as Potential Anticancer Agents. *Comput. Biol. Chem.* **2019**, *80*, 128–137.

(31) Su, L.; Zhang, H.; Yan, C.; Chen, A.; Meng, G.; Wei, J.; Yu, D.; Ding, Y. Superior Anti-Tumor Efficacy of Diisopropylamine Dichloroacetate Compared with Dichloroacetate in a Subcutaneous Transplantation Breast Tumor Model. *Oncotarget* **2016**, *7*, 65721–65731.

(32) Verma, A.; Lam, Y.-M.; Leung, Y.-C.; Hu, X.; Chen, X.; Cheung, E.; Tam, K. Y. Combined Use of Arginase and Dichloroacetate Exhibits Anti-Proliferative Effects in Triple Negative Breast Cancer Cells. *J. Pharm. Pharmacol.* **2018**, *71*, 306–315.

(33) Mayr, J.; Heffeter, P.; Groza, D.; Galvez, L.; Koellensperger, G.; Roller, A.; Alte, B.; Haider, M.; Berger, W.; Kowol, C. R.; Keppler, B. K.

An Albumin-Based Tumor-Targeted Oxaliplatin Prodrug with Distinctly Improved Anticancer Activity in vivo. *Chem. Sci.* **2017**, *8*, 2241–2250.

(34) Warnecke, A.; Fichtner, I.; Garmann, D.; Jaehde, U.; Kratz, F. Synthesis and Biological Activity of Water-Soluble Maleimide Derivatives of the Anticancer Drug Carboplatin Designed as Albumin-Binding Prodrugs. *Bioconjugate Chem.* **2004**, *15*, 1349–1359.

(35) Zheng, Y.-R.; Suntharalingam, K.; Johnstone, T. C.; Yoo, H.; Lin, W.; Brooks, J. G.; Lippard, S. J. Pt(IV) Prodrugs Designed to Bind Non-Covalently to Human Serum Albumin for Drug Delivery. *J. Am. Chem. Soc.* **2014**, *136*, 8790–8798.

(36) Moreau, B.; Alargova, R.; Brockman, A.; Whalen, K.; Quinn, J.; Meetze, K.; Bazinet, P.; DuPont, M.; Krawiec, B.; Kriksciukaite, K.; Lemelin, C.; LimSoo, P.; Oller, H.; Ramstack, M.; Rockwood, D.; Shinde, R.; Singh, S.; White, B.; AuYeung, T.; Dunbar, C.; Bilodeau, M.; Wooster, R. BTP-114: An Albumin Binding Cisplatin Prodrug with Improved and Sustained Tumor Growth Inhibition. *Cancer Res.* **2015**, *75*, 4484.

(37) Messori, L.; Merlino, A. Cisplatin Binding to Proteins: A Structural Perspective. *Coord. Chem. Rev.* **2016**, *315*, 67–89.

(38) Dhar, S.; Lippard, S. J. Structural and Mechanistic Studies of Anticancer Platinum Drugs: Uptake, Activation, and the Cellular Response to DNA Binding. *Platinum and Other Heavy Metal Compounds in Cancer Chemotherapy*; Humana Press, 2009; Vol. 3, pp 135–147.

(39) Karatoprak, G. Ş.; Küpeli Akkol, E.; Genç, Y.; Bardakçı, H.; Yücel, Ç.; Sobarzo-Sánchez, E. Combretastatins: An Overview of Structure, Probable Mechanisms of Action and Potential Applications. *Molecules* **2020**, *25*, 2560.

(40) Hura, N.; Sawant, A. V.; Kumari, A.; Guchhait, S. K.; Panda, D. Combretastatin-Inspired Heterocycles as Antitubulin Anticancer Agents. *ACS Omega* **2018**, *3*, 9754–9769.

(41) Kostrhunova, H.; Zajac, J.; Novohradsky, V.; Kasparkova, J.; Malina, J.; Aldrich-Wright, J. R.; Petruzzella, E.; Sirota, R.; Gibson, D.; Brabec, V. A Subset of New Platinum Antitumor Agents Kills Cells by a Multimodal Mechanism of Action Also Involving Changes in the Organization of the Microtubule Cytoskeleton. *J. Med. Chem.* **2019**, *62*, 5176–5190.

(42) Morrison, K. C.; Hergenrother, P. J. Whole Cell Microtubule Analysis by Flow Cytometry. *Anal. Biochem.* **2012**, *420*, 26–32.

(43) Kostrhunova, H.; Zajac, J.; Markova, L.; Brabec, V.; Kasparkova, J. A Multi-action Pt(IV) Conjugate with Oleate and Cinnamate Ligands Targets Human Epithelial Growth Factor Receptor HER2 in Aggressive Breast Cancer Cells. *Angew. Chem., Int. Ed. Engl.* **2020**, *59*, 21157–21162.

(44) Kostrhunova, H.; Petruzzella, E.; Gibson, D.; Kasparkova, J.; Brabec, V. An Anticancer Pt-IV Prodrug That Acts by Mechanisms Involving DNA Damage and Different Epigenetic Effects. *Chem.—Eur. J.* **2019**, *25*, 5235–5245.

(45) Brabec, V.; Hrabina, O.; Kasparkova, J. Cytotoxic Platinum Coordination Compounds. DNA Binding Agents. *Coord. Chem. Rev.* **2017**, *351*, 2–31.

(46) Wilson, J. J.; Lippard, S. J. Synthetic Methods for the Preparation of Platinum Anticancer Complexes. *Chem. Rev.* **2014**, *114*, 4470–4495.

(47) Novohradsky, V.; Zerkankova, L.; Stepankova, J.; Vrana, O.; Raveendran, R.; Gibson, D.; Kasparkova, J.; Brabec, V. Antitumor Platinum(IV) Derivatives of Oxaliplatin with Axial Valproate Ligands. *J. Inorg. Biochem.* **2014**, *140*, 72–79.

(48) Schmidt, C.; Karge, B.; Misgeld, R.; Prokop, A.; Franke, R.; Brönstrup, M.; Ott, I. Gold(I) NHC Complexes: Antiproliferative Activity, Cellular Uptake, Inhibition of Mammalian and Bacterial Thioredoxin Reductases, and Gram-Positive Directed Antibacterial Effects. *Chem.—Eur. J.* **2017**, *23*, 1869–1880.

(49) Ma, J.; Stoter, G.; Verweij, J.; Schellens, J. H. M. Comparison of Ethanol Plasma-Protein Precipitation with Plasma Ultrafiltration and Trichloroacetic Acid Protein Precipitation for the Measurement of Unbound Platinum Concentrations. *Cancer Chemother. Pharmacol.* **1996**, *38*, 391–394.